We have been examining SIVmac239 infection in multiple groups of Burmese rhesus macaques sharing MHC-I genotypes at the haplotype level and indicated an association of MHC-I haplotypes with AIDS progression [21,34]. In our previous study, a group of macaques sharing MHC-I haplotype *90-120-Ia* (A) induced dominant Gag-specific $CD8^+$ T-cell responses and tended to show slower disease progression after SIVmac239 challenge [21]. Prophylactic immunization of these A^+ macaques with a DNA vaccine prime and a Gag-expressing Sendai virus (SeV-Gag) vector boost resulted in SIV control based on Gag-specific $CD8^+$

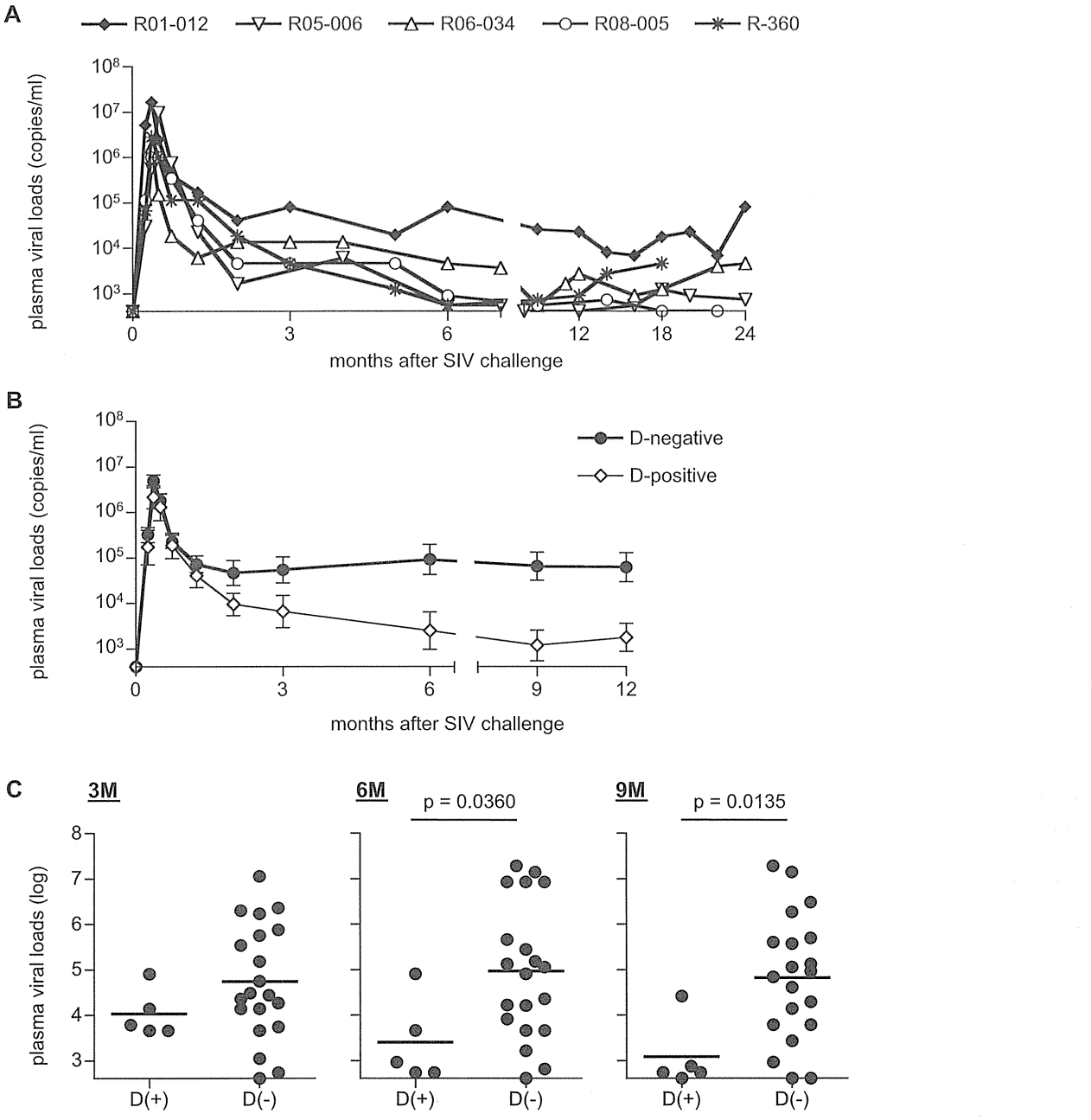

Figure 1. Plasma viral loads after SIVmac239 challenge in unvaccinated macaques. Plasma viral loads (SIV *gag* RNA copies/ml plasma) were determined as described previously [35]. The lower limit of detection is approximately 4×10^2 copies/ml. (A) Changes in plasma viral loads after challenge in unvaccinated macaques possessing MHC-I haplotype D. (B) Changes in geometric means of plasma viral loads after challenge in five unvaccinated D^+ animals in the present study and twenty D^- animals in our previous cohorts [21]. Three of twenty D^- animals were euthanized because of AIDS before 12 months, and we compared viral loads between D^+ and D^- animals until 12 months. (C) Comparison of plasma viral loads at 3 months (left panel), 6 months (middle panel), and 9 months (right panel) between the unvaccinated D^+ and the D^- animals. Viral loads at 6 months and 9 months in D^+ animals were significantly lower than those in the latter D^- animals ($p = 0.0360$ at 6 months and $p = 0.0135$ at 9 months by t-test).
doi:10.1371/journal.pone.0054300.g001

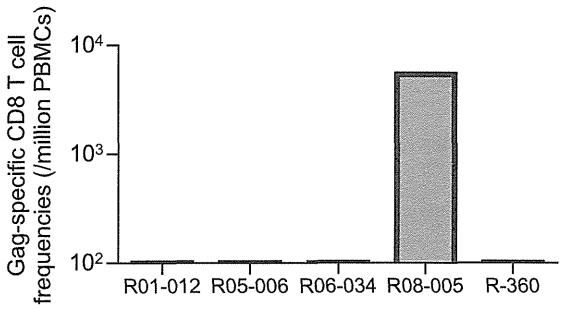

Figure 2. SIV Gag-specific CD8$^+$ T-cell responses in unvaccinated D$^+$ macaques at week 2 after SIVmac239 challenge.
doi:10.1371/journal.pone.0054300.g002

T-cell responses [35,36]. Accumulation of data on interaction between virus replication and T-cell responses in multiple groups of macaques sharing individual MHC-I haplotypes would provide great insights into our understanding of the mechanism for HIV/SIV control.

In the present study, we investigated SIVmac239 infection of a group of Burmese rhesus macaques possessing the MHC-I haplotype *90-010-Id* (D), which was not associated with dominant Gag-specific CD8$^+$ T-cell responses. These animals had persistent viremia in the early phase but showed significant reduction of viral loads around 6 months after SIV challenge. Most D$^+$ animals showed predominant Nef-specific but not Gag-specific CD8$^+$ T-cell responses. This study presents a protective MHC-I haplotype, indicating the potential of non-Gag antigen-specific CD8$^+$ T-cell responses to contribute to SIV control.

Materials and Methods

Ethics Statement

Animal experiments were carried out in National Institute of Biomedical Innovation (NIBP) and Institute for Virus Research in Kyoto University (IVRKU) after approval by the Committee on the Ethics of Animal Experiments of NIBP and IVRKU in accordance with the guidelines for animal experiments at NIBP, IVRKU, and National Institute of Infectious Diseases. To prevent viral transmission, animals were housed in individual cages allowing them to make sight and sound contact with one another, where the temperature was kept at 25°C with light in 12 hours per day. Animals were fed with apples and commercial monkey diet (Type CMK-2, Clea Japan, Inc. Tokyo). Blood collection, vaccination, and SIV challenge were performed under ketamine anesthesia. The endpoint for euthanasia was determined by typical signs of AIDS including reduction in peripheral CD4$^+$ T-cell counts (less than 200 cells/μl), 10% loss of body weight, diarrhea, and general weakness. At euthanasia, animals were deeply anesthetized with pentobarbital under ketamine anesthesia, and then, whole blood was collected from left ventricle.

Animal Experiments

We examined SIV infections in a group of Burmese rhesus macaques (n = 10) sharing the MHC-I haplotype *90-010-Id* (D). The determination of MHC-I haplotypes was based on the family study in combination with the reference strand-mediated conformation analysis (RSCA) of *Mamu-A* and *Mamu-B* genes and detection of major *Mamu-A* and *Mamu-B* alleles by cloning the reverse transcription (RT)-PCR products as described previously [21,34,37]. Macaques R01-012 and R01-009 used in our previous report [35] and macaques R03-021 and R03-016 used in an unpublished experiment were included in the present study. Five macaques R01-009, R06-020, R06-033, R03-021, and R03-016 received a prophylactic DNA prime/SeV-Gag boost vaccine (referred to as DNA/SeV-Gag vaccine) [35]. The DNA used for the vaccination, CMV-SHIVdEN, was constructed from an *env*-deleted and *nef*-deleted simian–human immunodeficiency virus SHIVMD14YE [38] molecular clone DNA (SIVGP1) and has the genes encoding SIVmac239 Gag, Pol, Vif, and Vpx, and HIV Tat and Rev. At the DNA vaccination, animals received 5 mg of CMV-SHIVdEN DNA intramuscularly. Six weeks after the DNA prime, animals received a single boost intranasally with 6×10^9 cell infectious units (CIUs) of F-deleted replication-defective SeV-Gag [39,40]. All animals were challenged intravenously with 1,000 $TCID_{50}$ (50 percent tissue culture infective doses) of SIVmac239 [41]. At week 1 after SIV challenge, macaque R03-021 was inoculated with nonspecific immunoglobulin G (IgG) and macaques R03-016 with IgG purified from neutralizing antibody-positive plasma of chronically SIV-infected macaques in our previous experiment [42].

Analysis of SIV Antigen-specific CD8$^+$ T-cell Responses

SIV antigen-specific CD8$^+$ T-cell responses were measured by flow-cytometric analysis of gamma interferon (IFN-γ) induction as described previously [43]. Autologous herpesvirus papio-immortalized B-lymphoblastoid cell lines (B-LCLs) were established from peripheral blood mononuclear cells (PBMCs) which were obtained from individual macaques before SIV challenge [44]. PBMCs obtained from SIV-infected macaques were cocultured with autologous B-LCLs pulsed with peptides or peptide pools using panels of overlapping peptides spanning the entire SIVmac239 Gag, Pol, Vif, Vpx, Vpr, Tat, Rev, Env, and Nef amino acid sequences. Alternatively, PBMCs were cocultured with B-LCLs infected with a vaccinia virus vector expressing SIVmac239 Gag for Gag-specific stimulation. Intracellular IFN-γ staining was performed using CytofixCytoperm kit (BD, Tokyo, Japan). Fluorescein isothiocianate-conjugated anti-human CD4 (BD), Peridinin chlorophyll protein (PerCP)-conjugated anti-human CD8 (BD), allophycocyanin Cy7 (APC-Cy7)-conjugated anti-human CD3 (BD), and phycoerythrin (PE)-conjugated anti-human IFN-γ antibodies (Biolegend, San Diego, CA) were used. Specific T-cell levels were calculated by subtracting non-specific IFN-γ$^+$ T-cell frequencies from those after peptide-specific stimulation. Specific T-cell levels less than 100 cells per million PBMCs were considered negative.

Sequencing Analysis of Plasma Viral Genomes

Viral RNAs were extracted using High Pure Viral RNA kit (Roche Diagnostics, Tokyo, Japan) from macaque plasma samples. Fragments of cDNAs encoding SIVmac239 Gag and Nef were amplified by nested RT-PCR from plasma RNAs and subjected to direct sequencing by using dye terminator chemistry and an automated DNA sequencer (Applied Biosystems, Tokyo, Japan) as described before [45]. Predominant non-synonymous mutations were determined.

Statistical Analysis

Statistical analysis was performed using Prism software version 4.03 with significance levels set at a P value of <0.050 (GraphPad Software, Inc., San Diego, CA). Plasma viral loads were log transformed and compared by an unpaired two-tailed t test.

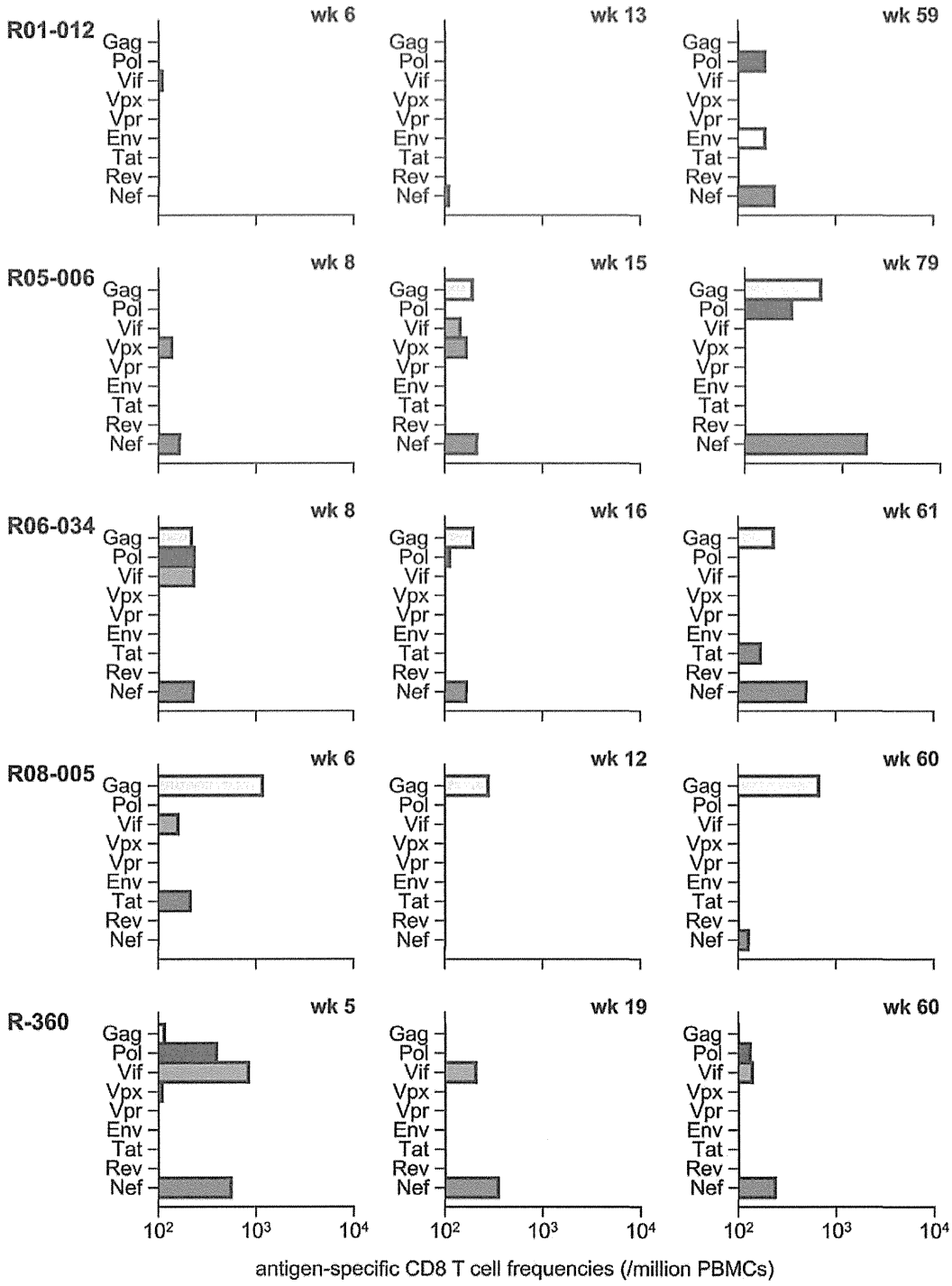

Figure 3. SIV antigen-specific CD8$^+$ T-cell responses in unvaccinated D$^+$ macaques. Responses were measured by the detection of antigen-specific IFN-γ induction in PBMCs obtained at indicated time points after SIVmac239 challenge.
doi:10.1371/journal.pone.0054300.g003

Results

Lower Viral Loads in D$^+$ Macaques in the Chronic Phase of SIV Infection

We first investigated SIVmac239 infection of five unvaccinated Burmese rhesus macaques sharing the MHC-I haplotype D (referred to as D$^+$ macaques). Confirmed MHC-I alleles consisting of this haplotype is *Mamu-A1*032:02*, *Mamu-B*004:01*, and *Mamu-B*102:01:01*. These animals showed lower set-point plasma viral loads (Fig. 1). Comparison of plasma viral loads between these five animals and our previous cohorts of SIVmac239-infected Burmese D-negative (D$^-$) rhesus macaques (n = 20) [21] revealed no

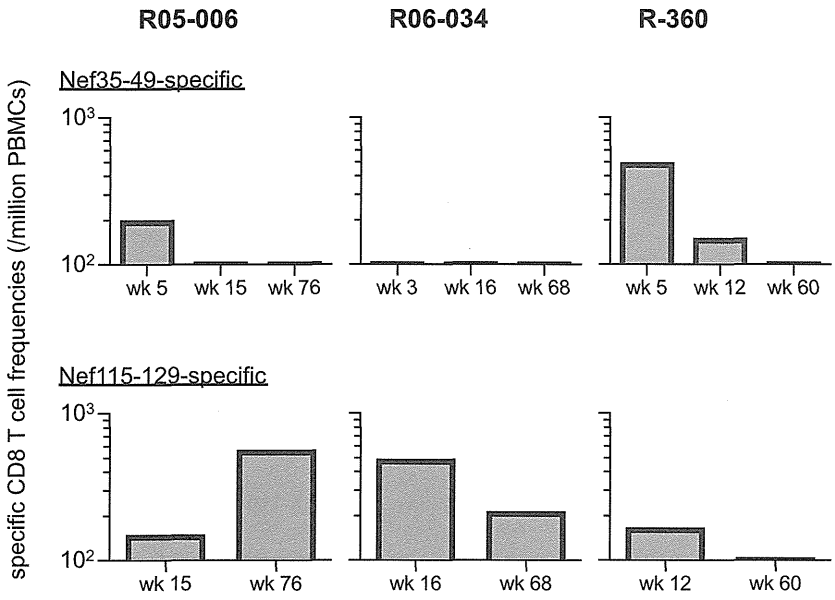

Figure 4. SIV Nef-specific CD8$^+$ T-cell responses in macaques R05-006, R06-034, and R-360. Nef_{35-49}-specific (upper panels) and $Nef_{115-129}$-specific (lower panels) CD8$^+$ T-cell responses were examined at indicated time points after SIVmac239 challenge.
doi:10.1371/journal.pone.0054300.g004

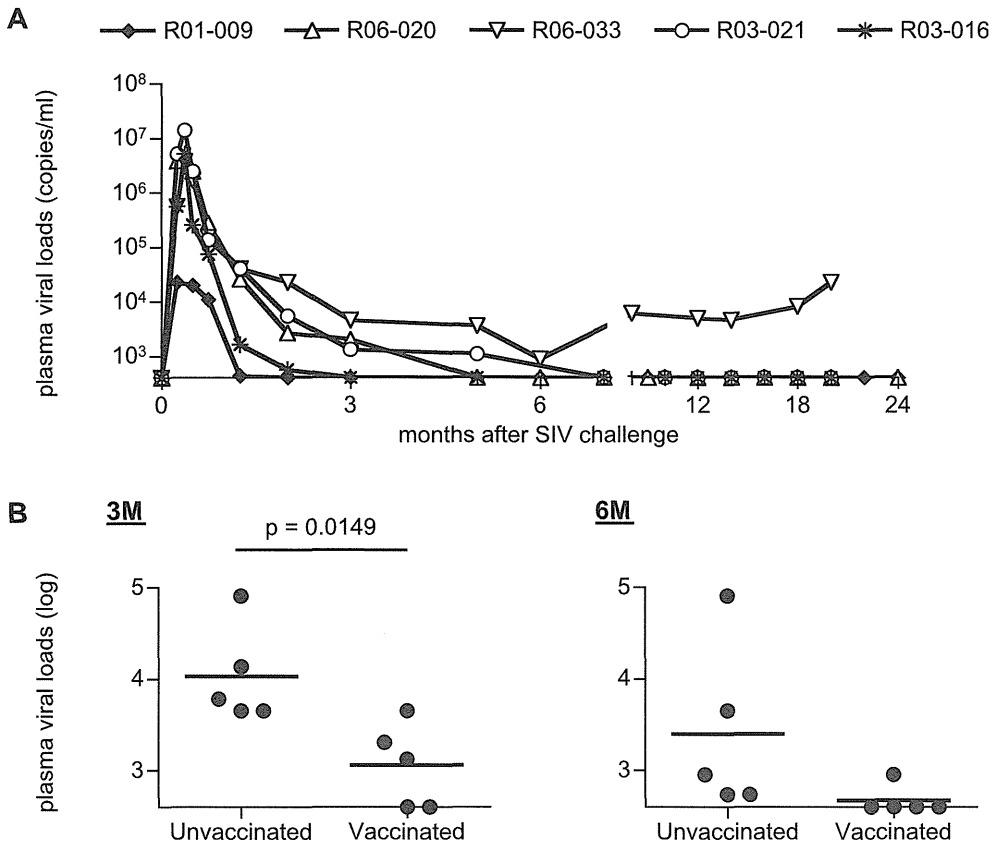

Figure 5. Plasma viral loads after SIVmac239 challenge in vaccinated D$^+$ macaques. (A) Changes in plasma viral loads after challenge vaccinated macaques possessing MHC-I haplotype D. (B) Comparison of plasma viral loads at 3 months (left panel) and 6 months (right panel) between five unvaccinated D$^+$ and five vaccinated D$^+$ animals. Viral loads at 3 months in vaccinated animals were significantly lower than those in the unvaccinated ($p = 0.0149$ by t-test).
doi:10.1371/journal.pone.0054300.g005

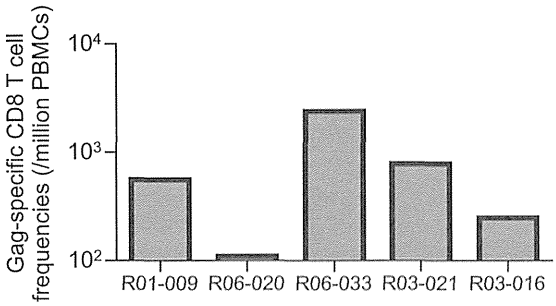

Figure 6. SIV Gag-specific CD8$^+$ T-cell responses in vaccinated D$^+$ macaques at week 2 after SIVmac239 challenge.
doi:10.1371/journal.pone.0054300.g006

significant difference at 3 months after SIV challenge ($p = 0.2436$ by t-test), but viral loads in the former D$^+$ animals became significantly lower than the latter after 6 months ($p = 0.0360$ at 6 months and $p = 0.0135$ at 9 months by t-test; Fig. 1). Four of these five macaques sharing MHC-I haplotype D showed low viral loads, less than 5×10^3 copies/ml, after 6 months, whereas macaque R01-012 maintained relatively higher viral loads.

Predominant Nef-specific CD8$^+$ T-cell Responses

We examined SIV antigen-specific CD8$^+$ T-cell responses by detection of antigen-specific IFN-γ induction. In the very acute phase, we did not have enough PBMC samples for measurement of individual SIV antigen-specific CD8$^+$ T-cell responses and focused on examining Gag-specific CD8$^+$ T-cell responses in most animals. At week 2 after challenge, Gag-specific CD8$^+$ T-cell responses were undetectable in four of five animals (Fig. 2).

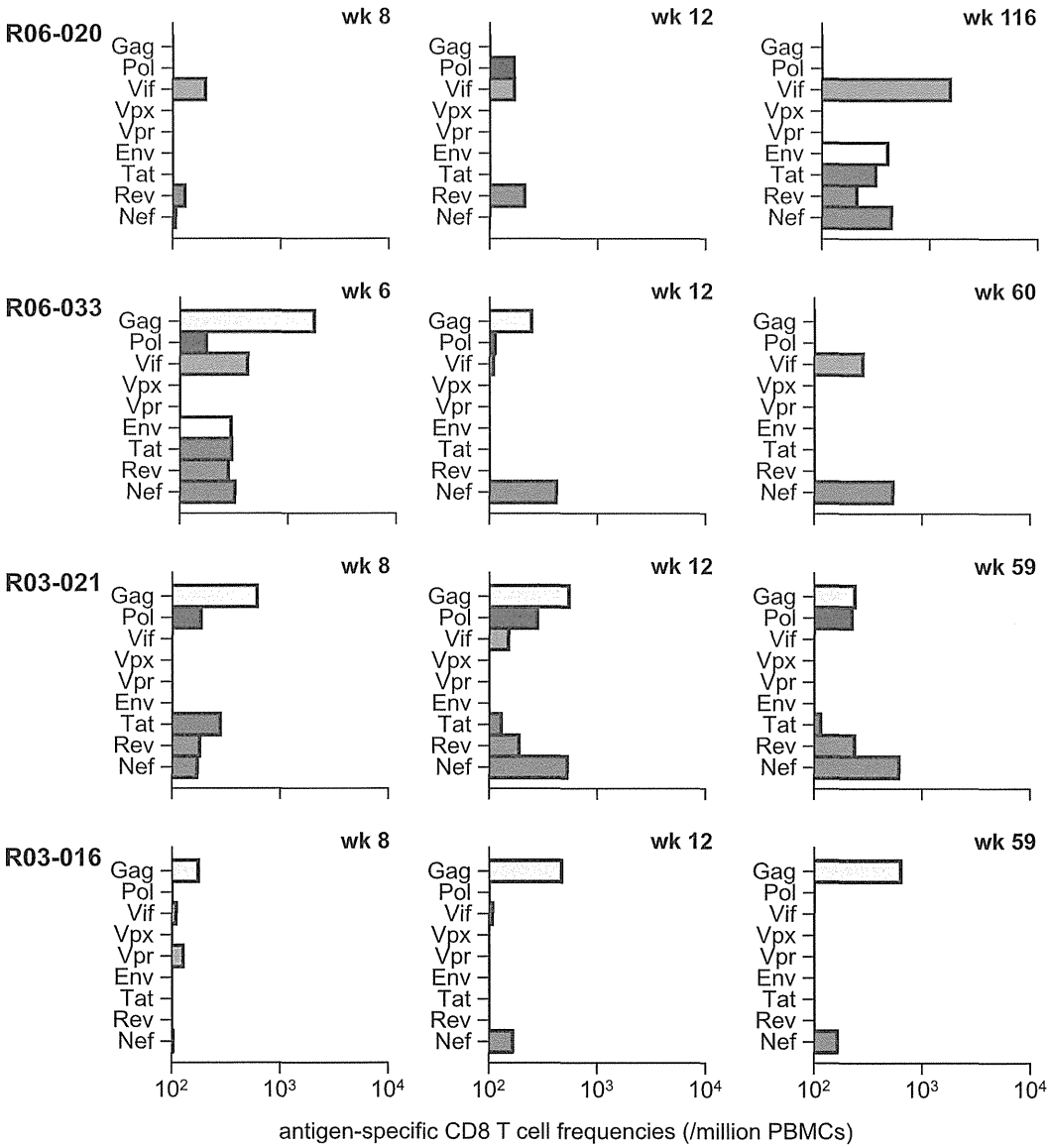

Figure 7. SIV antigen-specific CD8$^+$ T-cell responses in vaccinated D$^+$ animals after SIVmac239 challenge. Samples for this analysis were unavailable in macaque R01-009.
doi:10.1371/journal.pone.0054300.g007

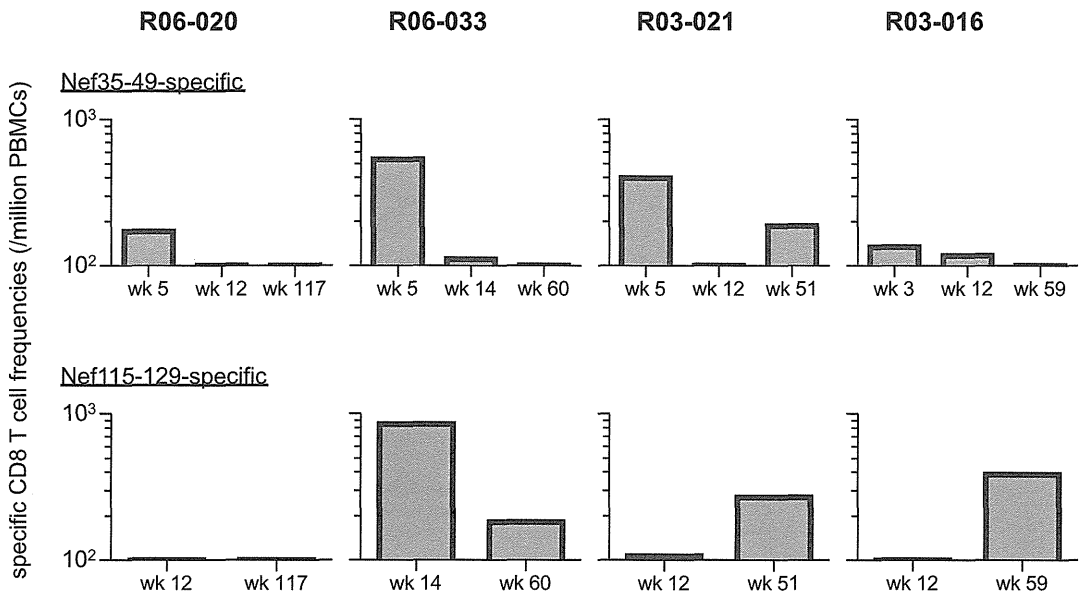

Figure 8. SIV Nef-specific CD8$^+$ T-cell responses in macaques R06-020, R06-033, R03-021, and R03-016. Nef_{35-49}-specific (upper panels) and $Nef_{115-129}$-specific (lower panels) CD8$^+$ T-cell responses were examined at indicated time points after SIVmac239 challenge.
doi:10.1371/journal.pone.0054300.g008

We then examined CD8$^+$ T-cell responses specific for individual SIV antigens in the early and the late phases (Fig. 3). Nef-specific but not Gag-specific CD8$^+$ T-cell responses were predominant in most D$^+$ animals. Gag-specific CD8$^+$ T-cell responses were dominantly induced in macaque R08-005 showing very low set-point viral loads. Macaque R01-012 having higher viral loads showed poor CD8$^+$ T-cell responses in the early phase.

Among four D$^+$ animals controlling SIV replication with less than 5×10^3 copies/ml of plasma viral loads after 6 months, Gag-specific CD8$^+$ T-cell responses were dominant only in macaque R08-005, while efficient Nef-specific CD8$^+$ T-cell responses were induced in the remaining three, suggesting possible contribution of Nef-specific CD8$^+$ T-cell responses to SIV control in these three controllers (R05-006, R06-034, and R-360). We then attempted to localize Nef CD8$^+$ T-cell epitopes shared in these animals and found Nef_{35-49}-specific and $Nef_{115-129}$-specific CD8$^+$ T-cell responses (Fig. 4), although we did not have enough samples for mapping the exact epitopes.

Reduction of Viral Loads in the Early Phase of SIV Infection by Prophylactic Vaccination

We also investigated SIVmac239 infection of additional five, vaccinated Burmese rhesus macaques sharing the MHC-I haplotype D. These animals received a prophylactic DNA/SeV-Gag vaccination. In four of these five vaccinated macaques, plasma viremia became undetectable after 6 months, while macaque R06-033 showed persistent viremia (Fig. 5A). Difference in viral loads between unvaccinated and vaccinated D$^+$ animals was unclear in the acute phase, but the latter vaccinees showed significant reduction in viral loads compared to those in the former unvaccinated at 3 months ($p = 0.0360$; Fig. 5B). After 6 months, unvaccinated animals also showed reduced viral loads, and the difference in viral loads between unvaccinated and vaccinated became unclear.

In contrast to unvaccinated D$^+$ animals, all five vaccinated animals elicited Gag-specific CD8$^+$ T-cell responses at week 2 after challenge (Fig. 6), reflecting the effect of prophylactic vaccination. We then examined CD8$^+$ T-cell responses specific for individual SIV antigens in these vaccinated animals (Fig. 7). Samples for this analysis were unavailable in vaccinated macaque R01-009. Vaccinated animals except for macaque R06-020 showed dominant Gag-specific CD8$^+$ T-cell responses even at 1–2 months. However, Gag-specific CD8$^+$ T-cell responses became not dominant after 1 year, while Nef-specific or Vif-specific CD8$^+$ T-cell responses became predominant, instead, in most vaccinees except for macaque R03-016.

Like three unvaccinated macaques (R05-006, R06-034, and R-360), vaccinated D$^+$ animals induced Nef_{35-49}-specific and $Nef_{115-129}$-specific CD8$^+$ T-cell responses after SIV challenge (Fig. 8). In analyses of three unvaccinated (Fig. 4) and four vaccinated animals (Fig. 8), Nef_{35-49}-specific CD8$^+$ T-cell responses were induced in the early phase in six animals but mostly became undetectable in the chronic phase. $Nef_{115-129}$-specific CD8$^+$ T-cell responses were also induced in most animals except for macaque R06-020 which showed $Nef_{112-126}$-specific ones in the chronic phase (data not shown). Macaques R05-006, R03-021, and R03-016 showed efficient $Nef_{115-129}$-specific CD8$^+$ T-cell responses not in the early phase but in the chronic phase. In contrast, vaccinated animal R06-033 that failed to control viremia showed higher $Nef_{115-129}$-specific CD8$^+$ T-cell responses in the early phase than those in the chronic phase.

Selection of Mutations in Nef CD8$^+$ T-cell Epitope-coding Regions

To see the effect of selective pressure by Nef-specific CD8$^+$ T-cell responses on viral genome mutations, we next analyzed nucleotide sequences in viral *nef* cDNAs amplified from plasma RNAs obtained at several time points after SIV challenge. Nonsynonymous mutations detected predominantly in Nef_{35-49}-coding and $Nef_{115-129}$-coding regions were as shown in Fig. 9. Remarkably, all the unvaccinated and vaccinated D$^+$ animals showed rapid selection of mutations in the Nef_{35-49}-coding region in 3 months. On the other hand, mutations in the $Nef_{115-129}$-coding region were observed in the late phase in all the three

		Nef35-49						Nef115-129				
Nef		36	37	41	42	44		119	122	124	125	126
		E	D	Q	S	G		M	F	K	E	K
R01-012	1M		*G									
	3M		*G									
	14M	*G	*G									
	24M	*G	*G			*E						
R05-006	1M					*E						
	3M			R								
	16M			R								
	24M			R								R
R06-034	1M											
	3M	*G										
	10M	*G	*G			*E						*R
	18M	G				E						R
R08-005	1M											
	3M				*F							
	6M	G										
	14M				F							
	24M	*G			F							
R-360	1M											
	3M		*G									
	6M		G									
	12M		G					T	L			
	20M		G					T	L			
R06-020	1M											
	3M	*K										
	11M		G	R								
R06-033	1M											
	3M	*G										
	6M		*G									
	14M		G			*E					K	E
R03-021	1M											
	3M				*F							
	14M	G								R		
R03-016	1M	*K		*R								
	4M	K										
	12M	K										

Figure 9. Predominant non-synonymous mutations in Nef_{35-49}-coding and $Nef_{115-129}$-coding regions of viral cDNAs in D^+ animals after SIVmac239 challenge. Amino acid substitutions are shown. Detection of similar levels of wild-type and mutant sequences at the residue is indicated by asterisks. Samples for this analysis were unavailable in macaque R01-009.
doi:10.1371/journal.pone.0054300.g009

unvaccinated animals eliciting $Nef_{115-129}$-specific $CD8^+$ T-cell responses. These mutations were also detected in two of three vaccinated animals eliciting $Nef_{115-129}$-specific $CD8^+$ T-cell responses.

We also analyzed viral *gag* sequences to see the effect of Gag-specific $CD8^+$ T-cell pressure on viral genome mutations in vaccinated animals (data not shown). Our previous study [35] showed rapid selection of a mutation leading to a glutamine (Q)-to-lysine (K) change at the 58th residue in Gag (Q58K) at week 5 in vaccinated macaque R01-009, although no more samples were available for this sequencing analysis. This Q58K mutation results in escape from Gag_{50-65}-specific $CD8^+$ T-cell recognition. In the present study, macaque R03-016 showed rapid selection of a mutation leading to a K-to-asparagine (N) change at the 478th residue in Gag in 1 month. These results may reflect rapid disappearance of detectable plasma viremia in 1 or 2 months in these two vaccinees. Macaque R06-020 showed selection of a *gag* mutation in 3 months, while other two vaccinees (R06-033 and R03-021) selected no *gag* mutation in the early phase.

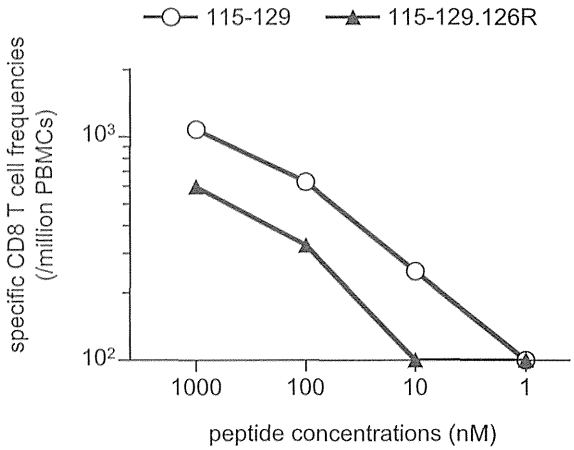

Figure 10. IFN-γ induction in $CD8^+$ T cells after stimulation with the wild-type or the mutant peptide. PBMCs obtained at week 31 from macaque R06-033 were stimulated by coculture with B-LCL pulsed with indicated concentrations of the wild-type $Nef_{115-129}$ peptide (open circles, 115–129, LAIDMSHFIKEKGGL) or the mutant $Nef_{115-129}$ peptide with a K126R alteration (closed triangles, 115–129.126R, LAIDMSHFIKERGGL).
doi:10.1371/journal.pone.0054300.g010

Discussion

HIV infection in humans with polymorphic MHC-I genotypes induces various patterns of viral antigen-specific $CD8^+$ T-cell responses. Previous studies have found several protective MHC-I alleles associated with lower viral loads and slower disease progression in HIV/SIV infection [7,13,14,16,17]. Elucidation of the mechanisms of viral control associated with individual protective MHC-I alleles would contribute to HIV cure and vaccine-based prevention. Because $CD8^+$ T-cell responses specific for some MHC-I-restricted epitopes can be affected by those specific for other MHC-I-restricted epitopes due to immunodominance [29,46,47], macaque groups sharing MHC-I genotypes at the haplotype level are useful for the analysis of cooperation of multiple epitope-specific $CD8^+$ T-cell responses. Previously, we reported a group of Burmese rhesus macaques sharing MHC-I haplotype *90-120-Ia* (A), which dominantly induce Gag-specific $CD8^+$ T-cell responses and tend to show slower disease progression after SIVmac239 challenge [21]. In the present study, we presented another type of protective MHC-I haplotype, which is not associated with dominant Gag-specific $CD8^+$ T-cell responses. Significant reduction of viral loads in unvaccinated macaques possessing this D haplotype compared to those in D^- macaques was observed after 6 months. Analysis of SIV infection in macaques sharing this protective MHC-I haplotype would lead to understanding of $CD8^+$ T-cell cooperation for viral control.

Analyses of antigen-specific $CD8^+$ T-cell responses after SIVmac239 challenge indicate that this MHC-I haplotype D is associated with predominant Nef-specific $CD8^+$ T-cell responses. Nef-specific $CD8^+$ T-cell responses were efficiently induced in all SIV controllers, whereas Gag-specific $CD8^+$ T-cell responses were dominant in only one of them. We found Nef_{35-49}-specific and $Nef_{115-129}$-specific $CD8^+$ T-cell responses shared in D^+ animals. We were unable to determine the MHC-I alleles restricting these epitopes, but these responses are not usually induced in our

previous D^- cohorts and considered to be associated with this MHC-I haplotype D.

Sequencing analysis of viral genomes showed rapid selection of mutations in the Nef_{36-44}-coding region within 3 months in all the D^+ animals. This is consistent with our results that Nef_{35-49}-specific $CD8^+$ T-cell responses were mostly induced in the early phase but undetectable in the chronic phase. These mutations were not consistently selected in our previous D^- cohorts and thus considered as MHC-I haplotype D-associated mutations. This suggests strong selective pressure by Nef_{35-49}-specific $CD8^+$ T-cell responses in the acute phase of SIVmac239 infection in D^+ macaques, although it remains undetermined whether these mutations result in viral escape from Nef_{35-49}-specific $CD8^+$ T-cell recognition.

$Nef_{115-129}$-specific $CD8^+$ T-cell responses were detected in six D^+ animals. In five of them, nonsynonymous mutations in the $Nef_{119-126}$-coding region were observed in the chronic phase. At least, we confirmed viral escape from $Nef_{115-129}$-specific $CD8^+$ T-cell recognition by a mutation leading to a K-to-arginine (R) (K126R) substitution at Nef residue 126 (Fig. 10). The number of nonsynonymous substitutions per the number of sites estimated to be nonsynonymous (dN) exceeded that estimated to be synonymous (dS) during the evolution process of $Nef_{115-129}$-coding region, but the value did not show statistically significant difference from that of neutral selection. Among three unvaccinated animals that controlled SIV replication without dominant Gag-specific $CD8^+$ T-cell responses, amino acid substitutions in the $Nef_{119-126}$-coding region were observed in a year in macaques R06-034 and R-360 but after 2 years in macaque R05-006. The former two animals tended to show earlier increases in plasma viral loads in the chronic phase, while the latter R05-006 maintained higher frequencies of $Nef_{115-129}$-specific $CD8^+$ T-cell responses. $Nef_{115-129}$-specific $CD8^+$ T-cell responses were efficient in the chronic phase in vaccinated controllers R03-021 and R03-016 but decreased in R06-033 that failed to contain SIV replication. Although a possible effect of this haplotype-associated factors other than $CD8^+$ T-cell responses such as NK activity on SIV infection [48,49,50] remains undetermined, these results imply involvement of Nef-specific $CD8^+$ T-cell responses in the SIV control associated with MHC-I haplotype D.

Unvaccinated macaque R08-005 dominantly elicited Gag antigen-specific $CD8^+$ T-cell responses and showed rapid selection of a mutation encoding Gag 257 residue, which was not observed in any other D^+ animals. Nef-specific $CD8^+$ T-cell responses were detectable only at week 2 in the acute phase (data not shown) and a mutation in the Nef_{42}-coding region was rapidly selected. It is speculated that those dominant Gag-specific $CD8^+$ T-cell responses associated with the second, non-D MHC-I haplotype were effective in this animal. Nef_{35-49}-specific $CD8^+$ T-cell responses may not be efficient due to immunodominance but exert some suppressive pressure on viral replication.

DNA/SeV-Gag vaccination resulted in earlier reduction of viral loads after SIV challenge. Vaccinees showed significantly lower viral loads at 3 months than those in unvaccinated animals. Gag-specific $CD8^+$ T-cell responses were elicited at week 2 in all the vaccinees but not in the unvaccinated except for one animal R08-005. No *gag* mutations were shared in the vaccinees in the acute phase, but three of them showed rapid selection of individual non-synonymous mutations in *gag*. Rapid selection of mutations in the Nef_{36-44}-coding region was consistently detected even in these vaccinees. These results suggest broader $CD8^+$ T-cell responses consisting of dominant vaccine antigen Gag-specific and inefficient naive-derived Nef-specific ones in the acute phase. In three vaccinated animals, Gag-specific $CD8^+$ T-cell responses became lower or undetectable, and instead, Nef-specific $CD8^+$ T-cell responses became predominant in the chronic phase.

In summary, we found a protective MHC-I haplotype not associated with dominant Gag-specific $CD8^+$ T-cell responses in SIVmac239 infection. Our results in D^+ macaques suggest suppressive pressure by Nef_{35-49}-specific and $Nef_{115-129}$-specific $CD8^+$ T-cell responses on SIV replication, contributing to reduction in set-point viral loads. DNA/SeV-Gag-vaccinated D^+ animals induced Gag-specific $CD8^+$ T-cell responses in addition to Nef-specific ones after SIV challenge, resulting in earlier containment of SIV replication. This study presents a pattern of SIV control with involvement of non-Gag antigen-specific $CD8^+$ T-cell responses, contributing to accumulation of our knowledge on HIV/SIV control mechanisms.

Acknowledgments

We thank F. Ono, K. Oto, K. Hanari, K. Komatsuzaki, M. Hamano, H. Akari, and Y. Yasutomi for their assistance in animal experiments.

Author Contributions

Performed animal experiments: HS TM TI YK. Performed MHC-I typing: TKN AK. Conceived and designed the experiments: NT TM. Performed the experiments: NT TN YT HY AT. Analyzed the data: NT HY T. Shiino TM. Contributed reagents/materials/analysis tools: MI AI HH T. Shu MH. Wrote the paper: NT TM.

References

1. Borrow P, Lewicki H, Hahn BH, Shaw GM, Oldstone MB (1994) Virus-specific CD8+ cytotoxic T-lymphocyte activity associated with control of viremia in primary human immunodeficiency virus type 1 infection. J Virol 68: 6103–6110.
2. Koup RA, Safrit JT, Cao Y, Andrews CA, McLeod G, et al. (1994) Temporal association of cellular immune responses with the initial control of viremia in primary human immunodeficiency virus type 1 syndrome. J Virol 68: 4650–4655.
3. Matano T, Shibata R, Siemon C, Connors M, Lane HC, et al. (1998) Administration of an anti-CD8 monoclonal antibody interferes with the clearance of chimeric simian/human immunodeficiency virus during primary infections of rhesus macaques. J Virol 72: 164–169.
4. Jin X, Bauer DE, Tuttleton SE, Lewin S, Gettie A, et al. (1999) Dramatic rise in plasma viremia after CD8+ T cell depletion in simian immunodeficiency virus-infected macaques. J Exp Med 189: 991–998.
5. Schmitz JE, Kuroda MJ, Santra S, Sasseville VG, Simon MA, et al. (1999) Control of viremia in simian immunodeficiency virus infection by CD8+ lymphocytes. Science 283: 857–860.
6. Carrington M, Nelson GW, Martin MP, Kissner T, Vlahov D, et al. (1999) HLA and HIV-1: heterozygote advantage and B*35-Cw*04 disadvantage. Science 283: 1748–1752.
7. Migueles SA, Sabbaghian MS, Shupert WL, Bettinotti MP, Marincola FM, et al. (2000) HLA B*5701 is highly associated with restriction of virus replication in a subgroup of HIV-infected long term nonprogressors. Proc Natl Acad Sci USA 97: 2709–2714.
8. Tang J, Tang S, Lobashevsky E, Myracle AD, Fideli U, et al. (2002) Favorable and unfavorable HLA class I alleles and haplotypes in Zambians predominantly infected with clade C human im- munodeficiency virus type 1. J Virol 76: 8276–8284.
9. Kiepiela P, Leslie AJ, Honeyborne I, Ramduth D, Thobakgale C, et al. (2004) Dominant influence of HLA-B in mediating the potential co-evolution of HIV and HLA. Nature 432: 769–775.
10. Leslie A, Matthews PC, Listgarten J, Carlson JM, Kadie C, et al. (2010) Additive contribution of HLA class I alleles in the immune control of HIV-1 infection. J Virol 84: 9879–9888.
11. Altfeld M, Addo MM, Rosenberg ES, Hecht FM, Lee PK, et al. (2003) Influence of HLA-B57 on clinical presentation and viral control during acute HIV-1 infection. AIDS 17: 2581–2591.
12. Altfeld M, Kalife ET, Qi Y, Streeck H, Lichterfeld M, et al. (2006) HLA alleles associated with delayed progression to AIDS contribute strongly to the initial CD8+ T cell response against HIV-1. PLoS Med 3: e403.
13. Goulder PJ, Watkins DI (2008) Impact of MHC class I diversity on immune control of immunodeficiency virus replication. Nat Rev Immunol 8: 619–630.

14. Muhl T, Krawczak M, Ten Haaft P, Hunsmann G, Sauermann U (2002) MHC class I alleles influence set-point viral load and survival time in simian immunodeficiency virus-infected rhesus monkeys. J Immunol 169: 3438–3446.
15. Mothe BR, Weinfurter J, Wang C, Rehrauer W, Wilson N, et al. (2003) Expression of the major histocompatibility complex class I molecule Mamu-A*01 is associated with control of simian immunodeficiency virus SIVmac239 replication. J Virol 77: 2736–2740.
16. Yant LJ, Friedrich TC, Johnson RC, May GE, Maness NJ, et al. (2006) The high-frequency major histocompatibility complex class I allele Mamu-B*17 is associated with control of simian immunodeficiency virus SIVmac239 replication. J Virol 80: 5074–5077.
17. Loffredo JT, Maxwell J, Qi Y, Glidden CE, Borchardt GJ, et al. (2007) Mamu-B*08-positive macaques control simian immunodeficiency virus replication. J Virol 81: 8827–8832.
18. Edwards BH, Bansal A, Sabbaj S, Bakari J, Mulligan MJ, et al. (2002) Magnitude of functional CD8+ T-cell responses to the gag protein of human immunodeficiency virus type 1 correlates inversely with viral load in plasma. J Virol 76: 2298–2305.
19. Zuniga R, Lucchetti A, Galvan P, Sanchez S, Sanchez C, et al. (2006) Relative dominance of Gag p24-specific cytotoxic T lymphocytes is associated with human immunodeficiency virus control. J Virol 80: 3122–3125.
20. Kiepiela P, Ngumbela K, Thobakgale C, Ramduth D, Honeyborne I, et al. (2007) CD8+ T-cell responses to different HIV proteins have discordant associations with viral load. Nat Med 13: 46–53.
21. Nomura T, Yamamoto H, Shiino T, Takahashi N, Nakane T, et al. (2012) Association of major histocompatibility complex class I haplotypes with disease progression after simian immunodeficiency virus challenge in Burmese rhesus macaques. J Virol 86: 6481–6490.
22. Schneidewind A, Brockman MA, Yang R, Adam RI, Li B, et al. (2007) Escape from the dominant HLA-B27-restricted cytotoxic T-lymphocyte response in Gag is associated with a dramatic reduction in human immunodeficiency virus type 1 replication. J Virol 81: 12382–12393.
23. Emu B, Sinclair E, Hatano H, Ferre A, Shacklett B, et al. (2008) HLA class I-restricted T-cell responses may contribute to the control of human immunodeficiency virus infection, but such responses are not always necessary for long-term virus control. J Virol 82: 5398–5407.
24. Miura T, Brockman MA, Schneidewind A, Lobritz M, Pereyra F, et al. (2009) HLA-B57/B*5801 human immunodeficiency virus type 1 elite controllers select for rare gag variants associated with reduced viral replication capacity and strong cytotoxic T-lymphocyte recognition. J Virol 83: 2743–2755.
25. Leslie AJ, Pfafferott KJ, Chetty P, Draenert R, Addo MM, et al. (2004) HIV evolution: CTL escape mutation and reversion after transmission. Nat Med 10: 282–289.
26. Martinez-Picado J, Prado JG, Fry EE, Pfafferott K, Leslie A, et al. (2006) Fitness cost of escape mutations in p24 Gag in association with control of human immunodeficiency virus type 1. J Virol 80: 3617–3623.
27. Crawford H, Prado JG, Leslie A, Hue S, Honeyborne I, et al. (2007) Compensatory mutation partially restores fitness and delays reversion of escape mutation within the immunodominant HLA-B*5703-restricted Gag epitope in chronic human immunodeficiency virus type 1 infection. J Virol 81: 8346–8351.
28. Friedrich TC, Valentine LE, Yant LJ, Rakasz EG, Piaskowski SM, et al. (2007) Subdominant CD8+ T-cell responses are involved in durable control of AIDS virus replication. J Virol 81: 3465–3476.
29. Loffredo JT, Bean AT, Beal DR, Leon EJ, May GE, et al. (2008) Patterns of CD8+ immunodominance may influence the ability of Mamu-B*08-positive macaques to naturally control simian immunodeficiency virus SIVmac239 replication. J Virol 82: 1723–1738.
30. Maness NJ, Yant LJ, Chung C, Loffredo JT, Friedrich TC, et al. (2008) Comprehensive immunological evaluation reveals surprisingly few differences between elite controller and progressor Mamu-B*17-positive simian immunodeficiency virus-infected rhesus macaques. J Virol 82: 5245–5254.
31. Valentine LE, Loffredo JT, Bean AT, Leon EJ, MacNair CE, et al. (2009) Infection with "escaped" virus variants impairs control of simian immunodeficiency virus SIVmac239 replication in Mamu-B*08-positive macaques. J Virol 83: 11514–11527.
32. Budde ML, Greene JM, Chin EN, Ericsen AJ, Scarlotta M, et al. (2012) Specific CD8+ T cell responses correlate with control of simian immunodeficiency virus replication in Mauritian cynomolgus macaques. J Virol 86: 7596–7604.
33. Mudd PA, Martins MA, Ericsen AJ, Tully DC, Power KA, et al. (2012) Vaccine-induced CD8+ T cells control AIDS virus replication. Nature 491: 129–133.
34. Naruse TK, Chen Z, Yanagida R, Yamashita T, Saito Y, et al. (2010) Diversity of MHC class I genes in Burmese-origin rhesus macaques. Immunogenetics 62: 601–611.
35. Matano T, Kobayashi M, Igarashi H, Takeda A, Nakamura H, et al. (2004) Cytotoxic T lymphocyte-based control of simian immunodeficiency virus replication in a preclinical AIDS vaccine trial. J Exp Med 199: 1709–1718.
36. Kawada M, Tsukamoto T, Yamamoto H, Iwamoto N, Kurihara K, et al. (2008) Gag-specific cytotoxic T-lymphocyte-based control of primary simian immunodeficiency virus replication in a vaccine trial. J Virol 82: 10199–10206.
37. Tanaka-Takahashi Y, Yasunami M, Naruse T, Hinohara K, Matano T, et al. (2007) Reference strand-mediated conformation analysis-based typing of multiple alleles in the rhesus macaque MHC class I Mamu-A and Mamu-B loci. Electrophoresis 28: 918–924.
38. Shibata R, Maldarelli F, Siemon C, Matano T, Parta M, et al. (1997) Infection and pathogenicity of chimeric simian-human immunodeficiency viruses in macaques: determinants of high virus loads and CD4 cell killing. J Infect Dis 176: 362–373.
39. Li HO, Zhu YF, Asakawa M, Kuma H, Hirata T, et al. (2000) A cytoplasmic RNA vector derived from nontransmissible Sendai virus with efficient gene transfer and expression. J Virol 74: 6564–6569.
40. Takeda A, Igarashi H, Nakamura H, Kano M, Iida A, et al. (2003) Protective efficacy of an AIDS vaccine, a single DNA priming followed by a single booster with a recombinant replication-defective Sendai virus vector, in a macaque AIDS model. J Virol 77: 9710–9715.
41. Kestler HW III, Ringler DJ, Mori K, Panicali DL, Sehgal PK, et al. (1991) Importance of the nef gene for maintenance of high virus loads and for development of AIDS. Cell 65: 651–662.
42. Yamamoto H, Kawada M, Takeda A, Igarashi H, Matano T (2007) Post-infection immunodeficiency virus control by neutralizing antibodies. PLoS One 2: e540.
43. Iwamoto N, Tsukamoto T, Kawada M, Takeda A, Yamamoto H, et al. (2010) Broadening of CD8+ cell responses in vaccine-based simian immunodeficiency virus controllers. AIDS 24: 2777–2787.
44. Voss G, Nick S, Stahl-Hennig C, Ritter K, Hunsmann G (1992) Generation of macaque B lymphoblastoid cell lines with simian Epstein-Barr-like viruses: transformation procedure, characterization of the cell lines and occurrence of simian foamy virus. J Virol Methods 39: 185–195.
45. Kawada M, Igarashi H, Takeda A, Tsukamoto T, Yamamoto H, et al. (2006) Involvement of multiple epitope-specific cytotoxic T-lymphocyte responses in vaccine-based control of simian immunodeficiency virus replication in rhesus macaques. J Virol 80: 1949–1958.
46. Tenzer S, Wee E, Burgevin A, Stewart-Jones G, Friis L, et al. (2009) Antigen processing influences HIV-specific cytotoxic T lymphocyte immunodominance. Nat Immunol 10: 636–646.
47. Ishii H, Kawada M, Tsukamoto T, Yamamoto H, Matsuoka S, et al. (2012) Impact of vaccination on cytotoxic T lymphocyte immunodominance and cooperation against simian immunodeficiency virus replication in rhesus macaques. J Virol 86: 738–745.
48. Flores-Villanueva PO, Yunis EJ, Delgado JC, Vittinghoff E, Buchbinder S, et al. (2001) Control of HIV-1 viremia and protection from AIDS are associated with HLA-Bw4 homozygosity. Proc Natl Acad Sci USA 98: 5140–5145.
49. Martin MP, Gao X, Lee JH, Nelson GW, Detels R, et al. (2002) Epistatic interaction between KIR3DS1 and HLA-B delays the progression to AIDS. Nat Genet 31: 429–434.
50. Martin MP, Qi Y, Gao X, Yamada E, Martin JN, et al. (2007) Innate partnership of HLA-B and KIR3DL1 subtypes against HIV-1. Nat Genet 39: 733–740.

JVI
Journals.ASM.org

No Viral Evolution in the Lymph Nodes of Simian Immunodeficiency Virus-Infected Rhesus Macaques during Combined Antiretroviral Therapy

Megu Oue, Saori Sakabe, Mariko Horiike, Mika Yasui, Tomoyuki Miura, Tatsuhiko Igarashi

Laboratory of Primate Model, Experimental Research Center for Infectious Diseases, Institute for Virus Research, Kyoto University, Kyoto, Japan

To elucidate the mode of viral persistence in primate lentivirus-infected individuals during combination antiretroviral therapy (cART), four simian immunodeficiency virus 239-infected monkeys were treated with cART for 1 year. The viral *env* genes prepared from total RNA extracted from the mesenteric lymph nodes collected at the completion of therapy were assessed by single genome amplification. Analyses of nucleotide substitutions and phylogeny revealed no viral evolution during cART.

Combination antiretroviral therapy (cART) has transformed human immunodeficiency virus (HIV) infection from an incurable disease to a manageable one. It suppresses the viral burden in patients to undetectable levels (1–3), lowers the chance of viral transmission (4), increases the number of $CD4^+$ T lymphocytes (1, 2), reconstitutes immunity (5–7), and extends the life expectancy of patients (8). However, cART does not cure patients because of its inability to eradicate the virus from infected individuals (9), suggesting the existence of a viral reservoir that is refractory to cART. Its identification and eradication are therefore requisites for a functional cure for AIDS. To establish a strategy for eradication of the HIV reservoir, the mechanism of persistence of the virus must be elucidated. Two mechanisms of viral persistence have been proposed: one is ongoing cycles of viral replication despite the presence of antivirals (10), and the other is provirus integration into long-lived cells (11). Whereas previous studies concerning this issue have been extensively conducted with clinical specimens from HIV-1-infected patients, including plasma, peripheral blood mononuclear cells, and gut-associated lymphatic tissues (12–14), lymph nodes, which are epicenters of virus replication in infected individuals not undergoing therapy (15–17), have only rarely been subjected to scrutiny. In animal models of cART, in particular, the simian immunodeficiency virus (SIV)-macaque model, which allows systemic examination, the location of the viral reservoir and the mechanism of viral holding have not been studied in detail.

To elucidate how the virus is maintained during cART in an animal model of anti-HIV chemotherapy, we administered a combination of nucleotide/nucleoside reverse transcriptase inhibitors (azidothymidine, lamivudine, and tenofovir disoproxil fumarate) and protease inhibitors (lopinavir with ritonavir) to four SIV239-infected rhesus macaques for 1 year (18). Although the plasma viral RNA loads of the animals were suppressed to levels below the assay detection limit during the period of chemotherapy, a systemic analysis conducted at the completion of therapy revealed viral RNA present in lymphatic tissues, especially in mesenteric and splenic lymph nodes (MLN and SLN, respectively) at high titers. Reasoning that any possible mode(s) of viral persistence should be in operation in tissues with high levels of viral RNA expression, we investigated viral genes in these tissues.

It is expected that viral genes accumulate nucleotide substitutions in proportion to the time postinfection in individuals not undergoing therapy because of continuous virus replication mediated by the error-prone viral reverse transcriptase. Such mutation rates have indeed been observed in the V3 loop of *env*, p17 of *gag* (19), and the C2-to-C5 region of *env* (20) in HIV-1-infected patients, as well as in the *env* gene from monkeys experimentally infected with SIV (21, 22). We hypothesized that viral genes would accumulate mutations if the virus was continuously replicating in the reservoir despite the presence of antivirals.

First, to ascertain whether such an accumulation of mutations took place at a detectable magnitude in our experimental system, we used SIV239, a molecularly cloned virus, to infect macaques for 1 year and periodically sampled viral genes from the untreated control animal (MM521). To reveal ongoing expression of viral genes at sampling, total RNA was extracted from plasma samples collected at 8, 18, 42, and 68 weeks postinfection (wpi) and examined. Single-genome amplification (SGA) (23) was used to amplify the viral genes present and to avoid the selective amplification of a particular genotype or recombination between genotypes during PCR. Using a nested PCR method, we amplified the entire *env* gene, which accumulates nucleotide substitutions in the greatest numbers, following reverse transcription of cDNA from the extracted RNA. The initial PCR cycles were carried out with the following primers: forward, SIV20F (5′-CTC CAG GAC TAG CAT AAA TGG-3′); reverse, SHenv9R (5′-GGG TAT CTA ACA TAT GCC TC-3′). Successive PCR cycles were run with the following primers: forward, SIV21F (5′-CTC TCT CAG CTA TAC CGC CC-3′); reverse, SHenv8R (5′-GCC TTC TTC CTT TTC TAA G-3′). The PCR products from an average of 12 independent reactions per time point were directly subjected to sequencing.

We computed the number of mutations in each SGA clone obtained from plasma samples of an untreated monkey (MM521) through a comparison with that of the inoculum virus (Fig. 1). A

Received 6 December 2012 Accepted 2 February 2013
Published ahead of print 13 February 2013
Address correspondence to Tatsuhiko Igarashi, tigarash@virus.kyoto-u.ac.jp.
Supplemental material for this article may be found at http://dx.doi.org/10.1128/JVI.03367-12.

doi:10.1128/JVI.03367-12

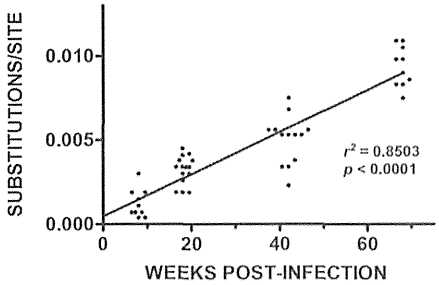

FIG 1 Time-dependent accumulation of nucleotide substitutions in SIV genomes circulating in an infected and untreated rhesus macaque. The sequences of viral *env* genes in circulation collected at 8, 18, 42, and 68 wpi from SIV239-infected animals and an untreated animal (MM521) were determined. Tamura-Nei distances (36) of the sequences were computed with the MEGA5 software (37), and the number of nucleotide substitutions per site was plotted against the number of weeks postinfection. Each symbol represents a single genomic amplicon derived from plasma samples collected at the time points designated.

linear relationship with a coefficient of 1.25×10^{-4} ($r^2 = 0.8503$, $P < 0.0001$; GraphPad Prism, La Jolla, CA) was revealed between the number of mutations in the SGA clones and the time postinfection. By using the coefficient, the cumulative number of mutations per annum was determined to be 6.5×10^{-3} substitutions/site/year, a value comparable to those of SIV and HIV reported previously (9×10^{-3} [21, 22] and 6.0×10^{-3} [23] substitutions/site/year, respectively). The accuracy of the "molecular clock" in our experimental setting prompted us to examine viral RNA extracted from the lymph nodes of animals that underwent cART for 1 year.

Total RNA was extracted from the MLN of four treated animals and one untreated animal, as well as the SLN of one of the treated animals (MM530), at the completion of the observation period and used as the template for PCR; the products were subjected to sequence analysis as described above. On average, 10 sequences were obtained from each sample (Fig. 2A and Table 1). The number of mutations observed in the *env* gene from MM521 (untreated) was, on average, 25 of 2,700 bases. In contrast, the number in treated animals was, on average, 1.5 of 2,700 bases (Table 1). The difference in the number of mutations in *env* between the plasma and MLN samples from the untreated animal, MM521, at 68 wpi (at necropsy) was statistically insignificant ($P > 0.05$; Fig. 2A), justifying our comparison of these two distinct anatomical compartments. Thus, we proceeded to compare the substitution numbers in plasma at 8 wpi, immediately before the onset of cART, with those from the lymph nodes of animals treated with cART at necropsy (61 to 65 wpi). The number of nucleotide substitutions in the *env* gene in both the plasma and MLN of the untreated animal (MM521) at 68 wpi was higher than that in plasma at 8 wpi ($P < 0.0001$). In contrast, those in the MLN of treated animals at the completion of cART were unchanged (MM528 and SLN of MM530) or decreased significantly (MM491, MM499, and MLN of MM530) (Fig. 2A). The results indicated that the virus did not accumulate further mutations beyond those obtained by 8 wpi.

As the samples were collected from animals at various time points postinfection, the numbers depicted in Fig. 2A were converted to substitutions/site/year (Fig. 2B) for further analysis. Comparison of the number of viral mutations in plasma at 8 wpi

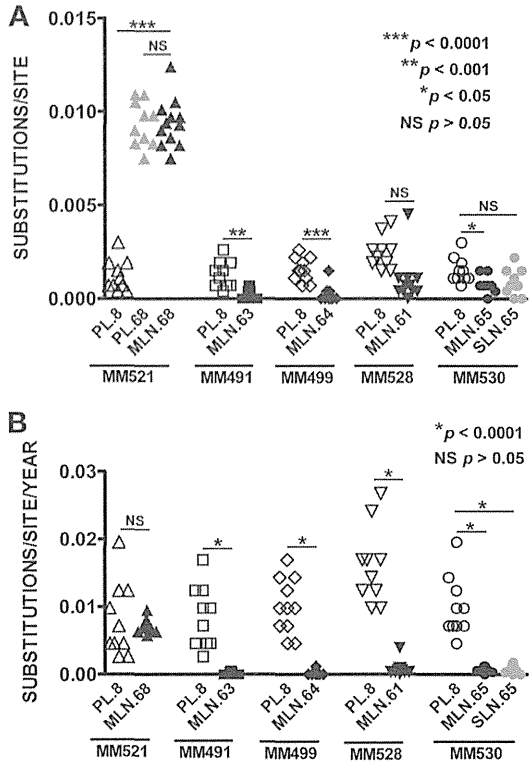

FIG 2 Nucleotide substitutions in *env* genes from SIV239-infected animals. The number of mutations in *env* from the plasma (PL, at 8 and 68 wpi) and MLN (at 68 wpi) of an SIV-infected but untreated animal (MM521) and from the plasma (at 8 wpi) and MLN (at necropsy, 61, 63, 64, or 65 wpi) and SLN (at necropsy, 65 wpi) from SIV-infected and treated monkeys (MM491, MM499, MM528, and MM530) were assessed as described in the legend to Fig. 1. (A) Numbers of nucleotide substitutions per site are shown. The statistical significance of differences between substitution numbers was evaluated by Student's *t* test using GraphPad Prism. *, $P < 0.05$; **, $P < 0.001$; ***, $P < 0.0001$; NS, $P > 0.05$. (B) Numbers of nucleotide substitutions per annum are shown. *, $P < 0.001$; NS, $P > 0.05$.

(median, 5.9×10^{-3} substitutions/site/year) with that in the MLN (median, 7.2×10^{-3} substitutions/site/year) in the untreated animal, MM521, indicated no statistically significant difference ($P = 0.6265$), as predicted by the analysis in Fig. 2A. Next, we compared the numbers in animals that underwent chemotherapy. At 8 wpi, the treated animals were equivalent to MM521 (an untreated animal) in terms of therapeutic status, since cART was started after sample collection at 8 wpi. Not unexpectedly, there was no statistically significant difference in the number of substitutions/site/year in plasma between the untreated and treated animals (MM491, 8.5×10^{-3}; MM499, 9.8×10^{-3}; MM528, 1.6×10^{-2}; MM530, 8.5×10^{-3}; MM521, 5.9×10^{-3}), except for MM528 ($P = 0.0048$ compared to the value for the untreated animal). In contrast, the number of mutations per annum in the lymph nodes of treated animals collected at necropsy (median, 3.4×10^{-4} substitutions/site/year) was significantly lower than that in the plasma of the animals at 8 wpi (median, 9.8×10^{-3} substitutions/site/year; $P < 0.0001$). The number of mutations per year in the lymph nodes also differed significantly between the untreated and treated macaques ($P < 0.0001$). This supports the hypothesis that ongoing viral replication contributed little, if anything, to viral persistence during cART.

TABLE 1 Origins and numbers of *env* clones

Animal (cART) and specimen	Sample collection time (wpi)	No. of SGA clones	No. of nucleotide substitutions	
			Minimum/ maximum	Mean ± SD
MM521 (untreated)				
Plasma	8	10	1/8	3.3 ± 2.2
Plasma	68	10	20/29	24.9 ± 3.2
MLN	68	12	20/33	25.0 ± 3.4
MM491 (treated)				
Plasma	8	10	1/7	3.5 ± 1.8
MLN	63	10	0/2	0.6 ± 0.8
MM499 (treated)				
Plasma	8	11	2/7	4.2 ± 1.7
MLN	64	10	0/4	0.7 ± 1.3
MM528 (treated)				
Plasma	8	10	4/11	6.6 ± 2.4
MLN	61	11	0/3 (12)[a]	1.7 ± 1.1[b]
MM530 (treated)				
Plasma	8	10	2/8	4.0 ± 1.7
MLN	65	10	0/4	2.1 ± 1.2
SLN	65	10	0/6	2.4 ± 1.9

[a] Interpreted as a hypermutant driven by APOBEC3G/F (Hypermut 2.0, http://www.hiv.lanl.gov/content/index).
[b] Computed excluding the clone with hypermutation.

Examination of the nucleotide substitution numbers did not indicate discernible *de novo* virus replication during cART. Therefore, we next investigated continuous viral replication during cART through phylogenetic analysis of viral *env* clones. Clones were obtained from the untreated animal (derived from plasma at 8, 18, 42, and 68 wpi and from MLN) and from one of the treated animals (derived from plasma at 8 wpi and from MLN at necropsy) (Fig. 3; see Fig. S1 in the supplemental material). To illustrate the accumulation and specific sites of mutations, Highlighter plot analysis (http://www.hiv.lanl.gov/content/sequence/HIGHLIGHT/help.html) was also performed. Phylogenetic analysis of the viral genes from the untreated animal revealed that (i) *env* clones from plasma exhibited increasing genetic distance from the inoculum virus with time; (ii) clones obtained at a given time point branched out of the one immediately before, a clear demonstration of viral evolution; and (iii) clones from lymph nodes formed a cluster with those from plasma collected at the same time. In contrast, clones from treated animals, regardless of the tissue origin or time point, formed a cluster with clones derived from the plasma of the untreated animal at 8 wpi and the inoculum virus (Fig. 3; see Fig. S1). The results of the Highlighter plot analysis were consistent with those of the phylogenetic analysis. These results clearly demonstrated that viral evolution did not take place in SIV239-infected rhesus macaques during cART. Analysis of the *env* genes in the peripheral blood

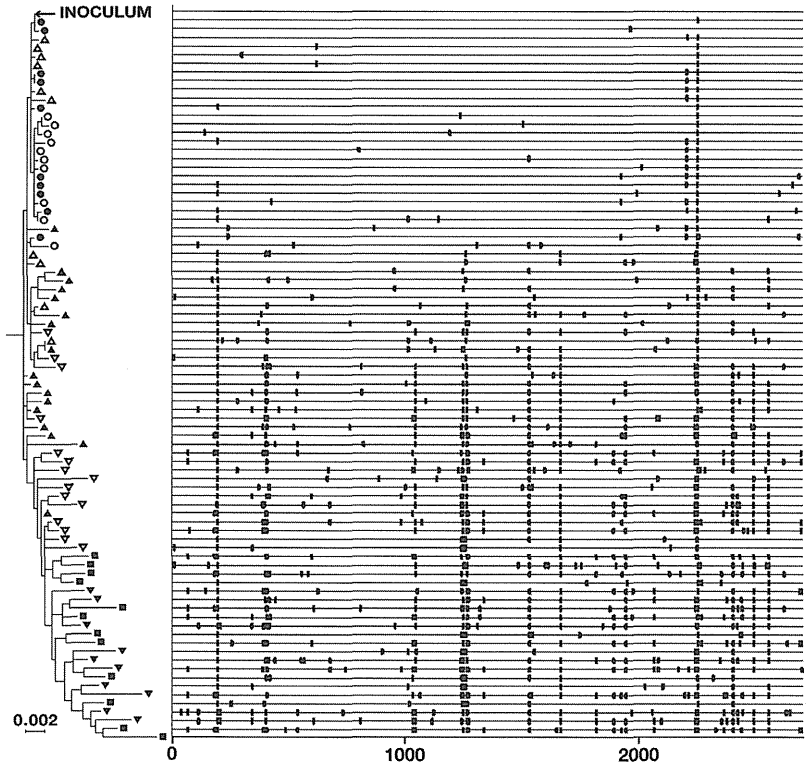

FIG 3 Phylogenetic relationship of *env* sequences from treated (MM530) and untreated (MM521) SIV-infected animals. Sequences of the entire *env* gene from both animals were subjected to phylogenetic analysis. The phylogenetic tree was constructed by the maximum-likelihood method (38). Open circles, sequences in the plasma of MM530 at 8 wpi; closed circles, those from the MLN of MM530 at 65 wpi; open triangles, those from plasma of MM521 at 8 wpi; closed triangles, those from plasma of MM521 at 18 wpi; open inverted triangles, those from plasma of MM521 at 42 wpi; closed inverted triangles, those from plasma of MM521 at 68 wpi; closed rectangles, those from MLN of MM521 at 68 wpi. The scale represents a genetic distance equivalent to 0.002 substitution/site. The corresponding sequence of SIVmac251 32H (GenBank accession no. D01065) was used as the outgroup.

mononuclear cells and gut-associated lymphatic tissues obtained from HIV-1 patients undergoing cART also found no evidence of *de novo* viral replication (13).

In contrast, other studies have reported continuous virus replication during combined chemotherapy (10, 12). One possible explanation for this discrepancy is the thorough suppression of the plasma viral burden, <20 copies/ml at necropsy, that was achieved in this study (18). *De novo* virus replication was detected in HIV-1-infected patients whose plasma viral RNA burdens ranged from 20 to 400 copies/ml but not in those with <20 copies/ml (24). Our findings also indicate that the cART regimen we used (18) was robust enough to halt viral evolution nearly completely in animals.

Our sample size, an average of 10 sequences from each specimen, may conceivably have limited our ability to detect minor populations with signs of ongoing replication. An analysis of four animals, however, did not reveal the genotypes detailed in the present study. Therefore, while our results cannot rule out possible *de novo* viral replication during cART, the data indicate that it is not a major mode of viral persistence in individuals whose virus replication levels are thoroughly suppressed by cART.

The locations of other potential viral reservoirs, in addition to resting $CD4^+$ T lymphocytes, an already established HIV/SIV reservoir found to be present in blood (25–28), lymph nodes (25), and the spleen (29), remains elusive. While the cART regimen we developed suppressed viral RNA levels nearly completely in the circulation and fairly well in effector sites, such as the gastrointestinal tract and lungs, viral RNA expression levels in lymph nodes were not contained effectively (18), suggesting that the viral reservoir consists of cells present in lymph nodes. We also detected CD3-positive cells, most likely $CD4^+$ T lymphocytes, expressing Nef protein in the follicles of the MLN of an SIV-infected animal that exhibited a viral rebound upon the cessation of cART (18). On the basis of their location, these might be Tfh cells, which are of the memory phenotype (30–32). The results of the present study have further narrowed the location of the viral reservoir from our previous study (18) to cells with longer half-lives that retain provirus for at least 1 year. Since resting $CD4^+$ T cells possess long half-lives (33), these cells satisfy this criterion for a viral reservoir during cART. It is conceivable that resting $CD4^+$ T cells functioned as the predominant viral reservoir in the SIV239-rhesus macaque model for patients undergoing cART employed in our study, as in preceding studies concerning the issue in the context of HIV and SIV infections.

Lymph nodes serve as a major HIV reservoir throughout the course of infection without intervention by cART (15–17). During clinical latency, the virus persists as an intact provirus, which can produce infectious viral particles upon cell activation, in a miniscule fraction of the resting $CD4^+$ T lymphocytes in lymph nodes (25). An extensive examination of lymph node specimens from HIV patients undergoing cART revealed an infinitesimal amount of viral RNA-positive cells by *in situ* hybridization (34). Hockett et al. (34) revealed that cART lowers the number of viral RNA-positive cells in lymph nodes but that the number of viral copies in each infected cell is constant, regardless of the viral burden in the circulation, suggesting the existence of virus-infected cells actively transcribing viral genes during cART, as we found previously in the lymph nodes of SIV239-infected animals undergoing cART (18). Our present observations, together with those of Hockett et al. (34), indicate that the viral RNA-positive cells present in lymph nodes during cART may represent cells infected with virus prior to the initiation of cART and transcribing viral RNA from integrated provirus during therapy.

Current cART is unable to eradicate the viral reservoir or, more precisely, provirus integrated in the reservoir. On the basis of our results, it is important to establish strategies to target specifically long-lived cells that harbor intact provirus while unlocking the dormant state of the provirus, perhaps by using histone deacetylase (35), to achieve a functional cure for AIDS.

ACKNOWLEDGMENTS

We are grateful to Tetsuro Matano for encouraging the initiation of this study, Beatrice H. Hahn for providing the protocol for SGA, and former and current members of the Igarashi laboratory for discussion and support.

This work was supported by Research on HIV/AIDS grants (H20-AIDS Research-003, H22-AIDS Research-007, and H24-AIDS Research-008) from The Ministry of Health, Labor and Welfare of Japan and by a Grant-in-Aid for Scientific Research (B) (23300156) from the Japan Society for the Promotion of Science.

REFERENCES

1. Gulick RM, Mellors JW, Havlir D, Eron JJ, Gonzalez C, McMahon D, Richman DD, Valentine FT, Jonas L, Meibohm A, Emini EA, Chodakewitz JA. 1997. Treatment with indinavir, zidovudine, and lamivudine in adults with human immunodeficiency virus infection and prior antiretroviral therapy. N. Engl. J. Med. 337:734–739.
2. Hammer SM, Squires KE, Hughes MD, Grimes JM, Demeter LM, Currier JS, Eron JJ, Jr, Feinberg JE, Balfour HH, Jr, Deyton LR, Chodakewitz JA, Fischl MA. 1997. A controlled trial of two nucleoside analogues plus indinavir in persons with human immunodeficiency virus infection and CD4 cell counts of 200 per cubic millimeter or less. AIDS Clinical Trials Group 320 Study Team. N. Engl. J. Med. 337:725–733.
3. Perelson AS, Essunger P, Cao Y, Vesanen M, Hurley A, Saksela K, Markowitz M, Ho DD. 1997. Decay characteristics of HIV-1-infected compartments during combination therapy. Nature 387:188–191.
4. Quinn TC, Wawer MJ, Sewankambo N, Serwadda D, Li C, Wabwire-Mangen F, Meehan MO, Lutalo T, Gray RH. 2000. Viral load and heterosexual transmission of human immunodeficiency virus type 1. Rakai Project Study Group. N. Engl. J. Med. 342:921–929.
5. Autran B, Carcelain G, Li TS, Blanc C, Mathez D, Tubiana R, Katlama C, Debre P, Leibowitch J. 1997. Positive effects of combined antiretroviral therapy on $CD4^+$ T cell homeostasis and function in advanced HIV disease. Science 277:112–116.
6. Pakker NG, Notermans DW, de Boer RJ, Roos MT, de Wolf F, Hill A, Leonard JM, Danner SA, Miedema F, Schellekens PT. 1998. Biphasic kinetics of peripheral blood T cells after triple combination therapy in HIV-1 infection: a composite of redistribution and proliferation. Nat. Med. 4:208–214.
7. Zhang ZQ, Notermans DW, Sedgewick G, Cavert W, Wietgrefe S, Zupancic M, Gebhard K, Henry K, Boies L, Chen Z, Jenkins M, Mills R, McDade H, Goodwin C, Schuwirth CM, Danner SA, Haase AT. 1998. Kinetics of $CD4^+$ T cell repopulation of lymphoid tissues after treatment of HIV-1 infection. Proc. Natl. Acad. Sci. U. S. A. 95:1154–1159.
8. Antiretroviral Therapy Cohort Collaboration. 2008. Life expectancy of individuals on combination antiretroviral therapy in high-income countries: a collaborative analysis of 14 cohort studies. Lancet 372:293–299.
9. Chun TW, Davey RT, Jr, Engel D, Lane HC, Fauci AS. 1999. Re-emergence of HIV after stopping therapy. Nature 401:874–875.
10. Wong JK, Hezareh M, Günthard HF, Havlir DV, Ignacio CC, Spina CA, Richman DD. 1997. Recovery of replication-competent HIV despite prolonged suppression of plasma viremia. Science 278:1291–1295.
11. Shen L, Siliciano RF. 2008. Viral reservoirs, residual viremia, and the potential of highly active antiretroviral therapy to eradicate HIV infection. J. Allergy Clin. Immunol. 122:22–28.
12. Anderson JA, Archin NM, Ince W, Parker D, Wiegand A, Coffin JM, Kuruc J, Eron J, Swanstrom R, Margolis DM. 2011. Clonal sequences recovered from plasma from patients with residual HIV-1 viremia and on intensified antiretroviral therapy are identical to replicating viral RNAs recovered from circulating resting $CD4^+$ T cells. J. Virol. 85:5220–5223.

13. Evering TH, Mehandru S, Racz P, Tenner-Racz K, Poles MA, Figueroa A, Mohri H, Markowitz M. 2012. Absence of HIV-1 evolution in the gut-associated lymphoid tissue from patients on combination antiviral therapy initiated during primary infection. PLoS Pathog. 8:e1002506. doi: 10.1371/journal.ppat.1002506.
14. Martínez MA, Cabana M, Ibanez A, Clotet B, Arno A, Ruiz L. 1999. Human immunodeficiency virus type 1 genetic evolution in patients with prolonged suppression of plasma viremia. Virology 256:180–187.
15. Embretson J, Zupancic M, Ribas JL, Burke A, Racz P, Tenner-Racz K, Haase AT. 1993. Massive covert infection of helper T lymphocytes and macrophages by HIV during the incubation period of AIDS. Nature 362: 359–362.
16. Pantaleo G, Graziosi C, Butini L, Pizzo PA, Schnittman SM, Kotler DP, Fauci AS. 1991. Lymphoid organs function as major reservoirs for human immunodeficiency virus. Proc. Natl. Acad. Sci. U. S. A. 88:9838–9842.
17. Pantaleo G, Graziosi C, Demarest JF, Butini L, Montroni M, Fox CH, Orenstein JM, Kotler DP, Fauci AS. 1993. HIV infection is active and progressive in lymphoid tissue during the clinically latent stage of disease. Nature 362:355–358.
18. Horiike M, Iwami S, Kodama M, Sato A, Watanabe Y, Yasui M, Ishida Y, Kobayashi T, Miura T, Igarashi T. 2012. Lymph nodes harbor viral reservoirs that cause rebound of plasma viremia in SIV-infected macaques upon cessation of combined antiretroviral therapy. Virology 423:107–118.
19. Leitner T, Albert J. 1999. The molecular clock of HIV-1 unveiled through analysis of a known transmission history. Proc. Natl. Acad. Sci. U. S. A. 96:10752–10757.
20. Shankarappa R, Margolick JB, Gange SJ, Rodrigo AG, Upchurch D, Farzadegan H, Gupta P, Rinaldo CR, Learn GH, He X, Huang XL, Mullins JI. 1999. Consistent viral evolutionary changes associated with the progression of human immunodeficiency virus type 1 infection. J. Virol. 73:10489–10502.
21. Burns DP, Desrosiers RC. 1991. Selection of genetic variants of simian immunodeficiency virus in persistently infected rhesus monkeys. J. Virol. 65:1843–1854.
22. Johnson PR, Hamm TE, Goldstein S, Kitov S, Hirsch VM. 1991. The genetic fate of molecularly cloned simian immunodeficiency virus in experimentally infected macaques. Virology 185:217–228.
23. Salazar-Gonzalez JF, Bailes E, Pham KT, Salazar MG, Guffey MB, Keele BF, Derdeyn CA, Farmer P, Hunter E, Allen S, Manigart O, Mulenga J, Anderson JA, Swanstrom R, Haynes BF, Athreya GS, Korber BT, Sharp PM, Shaw GM, Hahn BH. 2008. Deciphering human immunodeficiency virus type 1 transmission and early envelope diversification by single-genome amplification and sequencing. J. Virol. 82:3952–3970.
24. Günthard HF, Wong JK, Ignacio CC, Guatelli JC, Riggs NL, Havlir DV, Richman DD. 1998. Human immunodeficiency virus replication and genotypic resistance in blood and lymph nodes after a year of potent antiretroviral therapy. J. Virol. 72:2422–2428.
25. Chun TW, Carruth L, Finzi D, Shen X, DiGiuseppe JA, Taylor H, Hermankova M, Chadwick K, Margolick J, Quinn TC, Kuo YH, Brookmeyer R, Zeiger MA, Barditch-Crovo P, Siliciano RF. 1997. Quantification of latent tissue reservoirs and total body viral load in HIV-1 infection. Nature 387:183–188.
26. Chun TW, Finzi D, Margolick J, Chadwick K, Schwartz D, Siliciano RF. 1995. In vivo fate of HIV-1-infected T cells: quantitative analysis of the transition to stable latency. Nat. Med. 1:1284–1290.
27. Chun TW, Stuyver L, Mizell SB, Ehler LA, Mican JA, Baseler M, Lloyd AL, Nowak MA, Fauci AS. 1997. Presence of an inducible HIV-1 latent reservoir during highly active antiretroviral therapy. Proc. Natl. Acad. Sci. U. S. A. 94:13193–13197.
28. Finzi D, Hermankova M, Pierson T, Carruth LM, Buck C, Chaisson RE, Quinn TC, Chadwick K, Margolick J, Brookmeyer R, Gallant J, Markowitz M, Ho DD, Richman DD, Siliciano RF. 1997. Identification of a reservoir for HIV-1 in patients on highly active antiretroviral therapy. Science 278:1295–1300.
29. Shen A, Zink MC, Mankowski JL, Chadwick K, Margolick JB, Carruth LM, Li M, Clements JE, Siliciano RF. 2003. Resting $CD4^+$ T lymphocytes but not thymocytes provide a latent viral reservoir in a simian immunodeficiency virus-*Macaca nemestrina* model of human immunodeficiency virus type 1-infected patients on highly active antiretroviral therapy. J. Virol. 77:4938–4949.
30. Lindqvist M, van Lunzen J, Soghoian DZ, Kuhl BD, Ranasinghe S, Kranias G, Flanders MD, Cutler S, Yudanin N, Muller MI, Davis I, Farber D, Hartjen P, Haag F, Alter G, Schulze zur Wiesch J, Streeck H. 2012. Expansion of HIV-specific T follicular helper cells in chronic HIV infection. J. Clin. Invest. 122:3271–3280.
31. Lüthje K, Kallies A, Shimohakamada YT, Belz GT, Light A, Tarlinton DM, Nutt SL. 2012. The development and fate of follicular helper T cells defined by an IL-21 reporter mouse. Nat. Immunol. 13:491–498.
32. Weber JP, Fuhrmann F, Hutloff A. 2012. T-follicular helper cells survive as long-term memory cells. Eur. J. Immunol. 42:1981–1988.
33. Siliciano JD, Kajdas J, Finzi D, Quinn TC, Chadwick K, Margolick JB, Kovacs C, Gange SJ, Siliciano RF. 2003. Long-term follow-up studies confirm the stability of the latent reservoir for HIV-1 in resting $CD4^+$ T cells. Nat. Med. 9:727–728.
34. Hockett RD, Kilby JM, Derdeyn CA, Saag MS, Sillers M, Squires K, Chiz S, Nowak MA, Shaw GM, Bucy RP. 1999. Constant mean viral copy number per infected cell in tissues regardless of high, low, or undetectable plasma HIV RNA. J. Exp. Med. 189:1545–1554.
35. Archin NM, Liberty AL, Kashuba AD, Choudhary SK, Kuruc JD, Crooks AM, Parker DC, Anderson EM, Kearney MF, Strain MC, Richman DD, Hudgens MG, Bosch RJ, Coffin JM, Eron JJ, Hazuda DJ, Margolis DM. 2012. Administration of vorinostat disrupts HIV-1 latency in patients on antiretroviral therapy. Nature 487:482–485.
36. Tamura K, Nei M. 1993. Estimation of the number of nucleotide substitutions in the control region of mitochondrial DNA in humans and chimpanzees. Mol. Biol. Evol. 10:512–526.
37. Tamura K, Peterson D, Peterson N, Stecher G, Nei M, Kumar S. 2011. MEGA5: molecular evolutionary genetics analysis using maximum likelihood, evolutionary distance, and maximum parsimony methods. Mol. Biol. Evol. 28:2731–2739.
38. Felsenstein J. 1981. Evolutionary trees from DNA sequences: a maximum likelihood approach. J. Mol. Evol. 17:368–376.

JVI
Journals.ASM.org

Generation of Rhesus Macaque-Tropic HIV-1 Clones That Are Resistant to Major Anti-HIV-1 Restriction Factors

Masako Nomaguchi,[a] Masaru Yokoyama,[b] Ken Kono,[c] Emi E. Nakayama,[c] Tatsuo Shioda,[c] Naoya Doi,[a,d] Sachi Fujiwara,[a] Akatsuki Saito,[d,e] Hirofumi Akari,[e] Kei Miyakawa,[d,f] Akihide Ryo,[f] Hirotaka Ode,[d,g] Yasumasa Iwatani,[g] Tomoyuki Miura,[h] Tatsuhiko Igarashi,[h] Hironori Sato,[b] Akio Adachi[a]

Department of Microbiology, Institute of Health Biosciences, The University of Tokushima Graduate School, Tokushima, Tokushima, Japan[a]; Laboratory of Viral Genomics, Pathogen Genomics Center, National Institute of Infectious Diseases, Musashimurayama, Tokyo, Japan[b]; Department of Viral Infections, Research Institute for Microbial Diseases, Osaka University, Suita, Osaka, Japan[c]; Japanese Foundation for AIDS Prevention, Chiyoda-ku, Tokyo, Japan[d]; Section of Comparative Immunology and Microbiology, Center for Human Evolution Modeling Research, Primate Research Institute, Kyoto University, Inuyama, Aichi, Japan[e]; Department of Microbiology, Yokohama City University School of Medicine, Yokohama, Kanagawa, Japan[f]; Clinical Research Center, Department of Infectious Diseases and Immunology, National Hospital Organization Nagoya Medical Center, Nagoya, Aichi, Japan[g]; Laboratory of Primate Model, Experimental Research Center for Infectious Diseases, Institute for Virus Research, Kyoto University, Kyoto, Kyoto, Japan[h]

Human immunodeficiency virus type 1 (HIV-1) replication in macaque cells is restricted mainly by antiviral cellular APOBEC3, TRIM5α/TRIM5CypA, and tetherin proteins. For basic and clinical HIV-1/AIDS studies, efforts to construct macaque-tropic HIV-1 (HIV-1mt) have been made by us and others. Although rhesus macaques are commonly and successfully used as infection models, no HIV-1 derivatives suitable for *in vivo* rhesus research are available to date. In this study, to obtain novel HIV-1mt clones that are resistant to major restriction factors, we altered Gag and Vpu of our best HIV-1mt clone described previously. First, by sequence- and structure-guided mutagenesis, three amino acid residues in Gag-capsid (CA) (M94L/R98S/G114Q) were found to be responsible for viral growth enhancement in a macaque cell line. Results of *in vitro* TRIM5α susceptibility testing of HIV-1mt carrying these substitutions correlated well with the increased viral replication potential in macaque peripheral blood mononuclear cells (PBMCs) with different *TRIM5* alleles, suggesting that the three amino acids in HIV-1mt CA are involved in the interaction with TRIM5α. Second, we replaced the transmembrane domain of Vpu of this clone with the corresponding region of simian immunodeficiency virus SIVgsn166 Vpu. The resultant clone, MN4/LSDQgtu, was able to antagonize macaque but not human tetherin, and its Vpu effectively functioned during viral replication in a macaque cell line. Notably, MN4/LSDQgtu grew comparably to SIVmac239 and much better than any of our other HIV-1mt clones in rhesus macaque PBMCs. In sum, MN4/LSDQgtu is the first HIV-1 derivative that exhibits resistance to the major restriction factors in rhesus macaque cells.

Human immunodeficiency virus type 1 (HIV-1) has spread globally in human populations following cross-species transmission of simian immunodeficiency virus (SIV) from chimpanzees (1, 2). HIV-1 replicates well in humans and causes disease-inducing persistent infection only in humans. HIV-1 infection is impeded after virus entry in rhesus macaques (RhMs) and cynomolgus macaques (CyMs), which are frequently used for experimental viral infection studies (3). The block of HIV-1 infection in macaque cells is attributable to intrinsic restriction factors, including APOBEC3, TRIM5α/TRIM5CypA, and tetherin proteins (1, 4–6). These factors exert their antiretroviral activity in a species-specific manner, and HIV-1 effectively subverts their counterparts in human cells (1, 4–6). In contrast, a standard pathogenic clone, SIVmac239, for AIDS model studies evades the restriction factors and replicates well in macaques. HIV-1 and SIVmac239 are mutually related primate lentiviruses and cause AIDS in their respective hosts. Nevertheless, there are significant differences between the two viruses in genome organization, the viral replication profile *in vivo*, and disease progression (7–9). It is therefore most preferable to generate pathogenic HIV-1 derivatives to establish AIDS macaque models (7–9). Importantly, construction of HIV-1 derivatives that overcome the species barrier would contribute much to the understanding of the molecular interaction of viral and host proteins.

Of the intrinsic restriction factors in macaque cells, major determinants of the HIV-1 host range are the APOBEC3 and TRIM5 proteins (4, 8, 10). APOBEC3G is the strongest inhibitor of HIV-1 replication among APOBEC3 family proteins. It exhibits cytidine deaminase activity and causes hypermutation in the HIV-1 genome following incorporation into progeny virions in producer cells. HIV-1 Vif is able to degrade human APOBEC3G and neutralize its antiviral activity but is not effective against macaque APOBEC3G (4–6, 11, 12). Macaque TRIM5 proteins recognize and interact with the incoming HIV-1 cores and inhibit viral infection prior to reverse transcription (4, 6, 13, 14). TRIM5 proteins are composed of N-terminal RING, B-box 2, and coiled-coil domains. The C termini of TRIM5α and TRIM5CypA are the B30.2/SPRY and cyclophilin A (CypA) domains, respectively. All these domains in TRIM5 proteins are necessary to exert full restriction activity. Although the mechanism underlying TRIM5-mediated restriction has not been completely defined, inhibition of viral infection is initiated by capsid (CA) recognition with the

Received 7 June 2013 Accepted 9 August 2013
Published ahead of print 21 August 2013
Address correspondence to Hironori Sato, hirosato@nih.go.jp, or Akio Adachi, adachi@basic.med.tokushima-u.ac.jp.
M.N. and M.Y. contributed equally to this article.

doi:10.1128/JVI.01549-13

B30.2/SPRY or CypA domain. Sequence variation in the two domains determines species-specific restriction of retroviral infection. RhM *TRIM5* genes have been reported to be highly polymorphic (4, 6, 13, 14). Tetherin works as a virion release inhibition factor, and HIV-1 Vpu counteracts human but not macaque tetherin (4–6, 15). Tetherin may not be a potent barrier to limit cross-species transmission relative to APOBEC3G and TRIM5 proteins. However, tetherin antagonism is important for viral replication *in vivo*, because most primate lentiviruses have the ability to counteract tetherin, and tetherin-mediated restriction contributes to inhibiting viral replication *in vivo* (4, 5, 15). Recently, a novel anti-HIV-1 factor, SAMHD1, has been identified (4–6). Several Vpx and Vpr proteins appear to degrade SAMHD1 in a species-specific manner. However, SAMHD1 may be a weak species barrier, since HIV-1 has spread successfully and continuously in humans despite the lack of anti-SAMHD1 activity (4).

We and others have reported the construction of HIV-1 derivatives that have the ability to evade restriction factors for macaque model studies (16–21). As a common feature, all reported macaque-tropic HIV-1 (HIV-1mt) clones have the *vif* gene, which can neutralize macaque APOBEC3G (e.g., SIVmac239 *vif*). This modification is essential to evade APOBEC3G restriction and to gain the ability to replicate in macaque cells. To circumvent the restriction by TRIM5 proteins, two approaches have been taken. One approach is the use of pig-tailed macaques that do not express HIV-1-restrictive TRIM5 proteins. In this case, HIV-1 derivatives carrying authentic HIV-1 CA have been used as challenge viruses (stHIV-1_{SV} [16] and HSIV-vif [21]). Another approach is the replacement of the entire HIV-1 CA with the corresponding region of SIVmac239 (stHIV-1_{SCA+SV} [16, 17]). Although stHIV-1_{SCA+SV} replicates well in RhM cells, the CA region is not derived from HIV-1. Recently, chimeric viruses between simian-human immunodeficiency virus ($SHIV_{DH12}$ and $SHIV_{AD8}$) and an HIV-1 derivative (stHIV-1gsnU) that display anti-macaque tetherin activity have been reported (22, 23). However, the former construct is SHIV, and the latter is pig-tailed macaque-tropic HIV-1 carrying full-length SIVgsn71 (SIV from greater spot-nosed monkey) Vpu. While RhMs have been commonly and frequently used for viral infection experiments, no RhM-tropic HIV-1 derivatives that exhibit resistance to known major intrinsic restriction factors (APOBEC3, TRIM5, and tetherin proteins) have been reported.

We have previously described a unique HIV-1mt clone, designated MN4Rh-3, which can evade APOBEC3 and TRIM5CypA proteins but not TRIM5α and tetherin restrictions in macaque cells (Fig. 1) (19, 24). In this study, we generated new HIV-1mt clones from MN4Rh-3 that potentially possess an improved capacity to antagonize RhM TRIM5α and tetherin proteins. First, we constructed a number of MN4Rh-3 CA mutant clones; examined their growth potentials in an RhM lymphocyte cell line, M1.3S (25); and selected a new HIV-1mt clone, MN4/LSDQ, carrying only three amino acid substitutions in MN4Rh-3 CA (Fig. 1). MN4/LSDQ exhibited enhanced growth potential accompanied by increased resistance to macaque TRIM5α restriction. Next, we replaced the transmembrane (TM) domain of MN4/LSDQ Vpu with the corresponding region of SIVgsn166 (another SIVgsn) Vpu, which shows anti-macaque tetherin activity (26). The resultant clone, MN4/LSDQgtu, gained the ability to antagonize specifically macaque tetherin (Fig. 1). The replication efficiency of MN4/LSDQgtu in RhM peripheral blood mononuclear cells (PBMCs) was comparable to that of SIVmac239 and was superior to those of the other HIV-1mt clones (MN4Rh-3 and MN4/LSDQ). MN4/LSDQgtu is the first HIV-1 derivative that is highly resistant to the known major restriction factors (APOBEC3, TRIM5, and tetherin proteins) in RhM cells. Generation of MN4/LSDQgtu also served to find amino acid residues in CA involved in the interaction with macaque TRIM5α and to verify HIV-1mt growth enhancement in macaque cells by macaque tetherin antagonism.

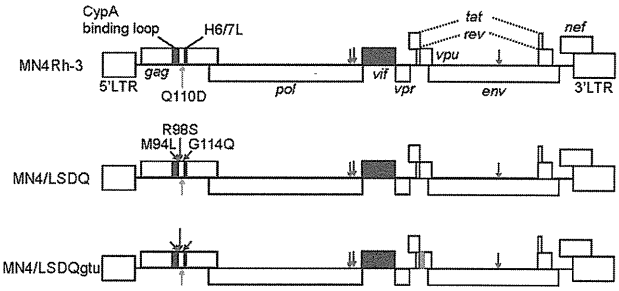

FIG 1 Proviral genome structures of various HIV-1mt clones. HIV-1 NL4-3 (32), SIVmac239 MA239 (71), and SIVgsn166 (GenBank accession number AF468659) sequences are indicated by white, black, and red areas, respectively. Green arrows show adaptive mutations that enhance viral growth potential (47). Orange arrows show the CA-Q110D mutation that augments viral growth in macaque cells/monkeys (19, 24). Blue arrows indicate CA substitutions (M94L/R98S/G114Q) identified in this study that are responsible for viral growth enhancement. H6/7L, loop between helices 6 and 7 in Gag-CA.

MATERIALS AND METHODS

Cells. An RhM lymphocyte cell line, M1.3S (25), was maintained in RPMI 1640 medium containing 10% heat-inactivated fetal bovine serum (FBS) and 50 units/ml of recombinant human interleukin-2 (IL-2) (Bio-Rad Laboratories Inc., Hercules, CA). The human monolayer cell lines 293T (27) and HEp2 (ATCC CCL-23) and the RhM kidney cell line LLC-MK2 (ATCC CCL-7) were maintained in Eagle's minimal essential medium (MEM) containing 10% FBS. MAGI cells (28) were cultured in MEM containing 10% FBS, 200 μg/ml G418 (Sigma-Aldrich Co., St. Louis, MO), and 100 μg/ml hygromycin B (Sigma-Aldrich Co.).

Plasmid DNA. The construction of MN4Rh-3, SIVmac239 clone MA239N, and its *nef*-deficient variant MA239N-ΔN was described previously (19, 25). CA alterations of HIV-1mt proviral clones were performed by replacing target sites of HIV-1mt CA with the corresponding sites of SIVmac239 (both codons and amino acids were changed to those of SIVmac239) by using the QuikChange site-directed mutagenesis kit (Agilent Technologies Inc., Santa Clara, CA). MN4/LSDQ was generated by introducing the following codon/amino acid substitutions into MN4Rh-3 (uppercase letters represent amino acids and lowercase letters represent codons): M(atg) to L(ctt) at amino acid position 94, R(agg) to S(tca) at position 98, and G(gga) to Q(cag) at position 114. Each *vpu* gene of SIVmon (SIV from mona monkey)/SIVmus (SIV from mustached monkey)/SIVgsn (SIVmon/mus/gsn) was synthesized (TaKaRa Bio Inc., Otsu, Japan) and cloned into pSG-cFLAG to express mon-, mus-, and gsn-Vpu, respectively, as described previously (29). Full-length Vpu sequences composed of the TM domain of SIVmon/mus/gsn Vpu and the cytoplasmic domain of HIV-1_{NL4-3} Vpu (monTM-, musTM-, and gsnTM-Vpu, respectively) were made by overlapping PCR and inserted into the pSG-cFLAG expression vector, as described previously (29). The resultant clones were designated pSG-VpucFLAG constructs. RhM and human tetherin sequences were amplified by PCR using cDNAs from M1.3S cells and HeLa cells, respectively. The amplified products were cloned into the pCIneo vector (Promega Corporation, Madison, WI) to generate pCIneo-RhM tetherin and pCIneo-Human tetherin. The sequence of RhM tetherin from M1.3S cells was identical to that of an RhM

tetherin variant [Mac(m)3] (30, 31). For flow cytometry analysis, pIRES-HIV-1-Vpu-hrGFP and pIRES-gsnTM-Vpu-hrGFP were constructed as described previously (29). The MN4/LSDQdtu clone was constructed by replacing the TM domain of MN4/LSDQ Vpu with the corresponding region of HIV-1_{DH12} Vpu (22) by using the QuikChange site-directed mutagenesis kit (Agilent Technologies Inc.). The MN4/LSDQgtu clone was generated by overlapping PCR between MN4/LSDQ and gsnTM-Vpu. *vpu*-deficient HIV-1mt clones were constructed by changing the initiation codon (ATG) to AGG and the second codon of each construct to TAG (stop codon).

Virus stocks and reverse transcriptase assay. Virus stocks were prepared from 293T cells transfected with proviral clones by the calcium-phosphate coprecipitation method (32). Virion-associated reverse transcriptase (RT) activity was measured as described previously (33), with the following modifications: 5 μl of culture supernatant was mixed with 25 μl of an RT reaction mixture containing a template primer of poly(A) (500 μg/ml; Midland Certified Reagent Company Inc., Midland, TX) and oligo(dT)$_{12-18}$ (1.25 μg/ml; New England BioLabs Inc., Ipswich, MA) in 50 mM Tris (pH 7.8), 75 mM KCl, 2 mM dithiothreitol, 5 mM $MgCl_2$, 0.05% Nonidet P-40, and 9.25 kBq of [α-^{32}P]dTTP (29.6 TBq/mmol; Perkin-Elmer Inc., Waltham, MA). After incubation at 37°C for 3 h, 10 μl of the reaction mixture was spotted onto DE81 anion-exchange paper (GE Healthcare UK Ltd., Buckinghamshire, England) and washed four times with 2× SSC (0.3 M NaCl plus 0.03 M sodium citrate) to remove unincorporated [α-^{32}P]dTTP. Spots were then counted with a scintillation counter.

Virus replication assays. Virus replication in M1.3S cells was monitored as described previously (25). For infection of macaque primary cells, RhM and CyM PBMCs were separated by Ficoll-Paque Plus (GE Healthcare UK Ltd.) and stimulated with RPMI 1640 medium containing 10% FBS, 50 units/ml of recombinant human IL-2, and 2 μg/ml of phytohemagglutinin L (PHA-L) (Roche Diagnostics GmbH, Mannheim, Germany). Primary PBMCs without CD8$^+$ cell depletion were used in this study. On day 3 poststimulation, cells were spin infected (34) with equal amounts of viruses prepared from transfected 293T cells and cultured in the presence of IL-2. Viral growth was monitored by RT activity released into the culture supernatants. The genotype of *TRIM5* alleles was analyzed as described previously (35).

TRIM5α susceptibility assays. Assays using recombinant Sendai virus (SeV)-RhM TRIM5α and SeV-CyM TRIM5α expression systems were performed as described previously (36). MT4 cells (10^5) were infected with SeV expressing each TRIM5α at a multiplicity of infection of 10 PFU per cell and incubated at 37°C for 9 h. Cells were then superinfected with HIV-1mt derivatives (20 ng of Gag-p24) or SIVmac239 (20 ng of Gag-p27). Culture supernatants were collected at intervals, and the amount of Gag-p24 or Gag-p27 produced was determined by using RETROtek antigen enzyme-linked immunosorbent assay (ELISA) kits (ZeptoMetrix Corporation, Buffalo, NY).

Virion release assays. Tetherin-null 293T cells were used for virion release assays. For analysis of Vpu expression vectors, subconfluent 293T cells in 24-well dishes were cotransfected with *vpu*-deficient MN4Rh-3 (300 ng), pCIneo-RhM tetherin (5 ng), and various pSG-VpucFLAG vectors (200 ng) by using Lipofectamine 2000 (Life Technologies Corporation, Carlsbad, CA). On day 2 posttransfection, virion production in the cell culture supernatants was measured by RT assays. For analysis of proviral clones, 700 ng of MA239N/MA239N-ΔN or 300 ng of MN4 derivatives and an appropriate amount of pCIneo-RhM tetherin or pCIneo-Human tetherin were used for cotransfection.

Flow cytometry analysis. Flow cytometry analysis was performed to examine cell surface CD4 or tetherin downregulation by Vpu, as described previously (29). For analysis of cell surface CD4, MAGI cells in 60-mm dishes were transfected with pIRES-hrGFP-Vpu vectors. On day 2 posttransfection, cells were trypsinized, washed with phosphate-buffered saline (PBS), and resuspended in PBS containing 10% FBS. Cells were then stained with a phycoerythrin (PE)-conjugated mouse anti-human CD4 antibody (BD Biosciences, San Jose, CA). For analysis of cell surface tetherin, LLC-MK2 or HEp2 cells in 60-mm dishes were transfected with pIRES-hrGFP-Vpu vectors and harvested as described above. Cells were then reacted with an anti-HM1.24 monoclonal antibody (a generous gift from Chugai Pharmaceutical Co. Ltd., Chuo-ku, Japan) and stained with a secondary PE-conjugated anti-mouse Ig antibody (BD Biosciences). Stained cells were analyzed with a FACSCalibur instrument using CELLQuest software (BD Biosciences).

Prediction of the effects of amino acid substitutions on the stability of the HIV-1mt CA N-terminal domain. The three-dimensional (3-D) model of the HIV-1mt CA N-terminal domain (NTD) was constructed by homology modeling using "MOE-Align" and "MOE-Homology" in the Molecular Operating Environment (MOE) (Chemical Computing Group Inc., Quebec, Canada) and refined as described previously (19). The crystal structure of the HIV-1 CA NTD at a resolution of 2.00 Å (Protein Data Bank [PDB] accession number 1M9C) (37) was used as the modeling template. The changes in the stability of the CA NTD by mutations were computed by using the Protein Design application in MOE. Single-point mutations on the CA protein were generated, and ensembles of protein conformations were generated by using the LowMode MD module in MOE to calculate average stability using Boltzmann distribution. Finally, the stability scores of the structures refined by energy minimization were obtained through the stability scoring function of the Protein Design application.

Structural modeling of the Vpu TM domains. We first constructed 3-D structural models for monomers of Vpu TM domains encoded in three HIV-1mt clones (MN4/LSDQ, MN4/LSDQdtu, and MN4/LSDQgtu) with PyMOL on the basis of the previously reported structure of the HIV-1_{BH10} Vpu TM domain (PDB accession number 1PI8) (38). The HIV-1_{BH10} Vpu TM domain has a sequence identical to that of the MN4/LSDQ Vpu TM domain. The 3-D structures of their tetramers were then predicted from the constructed monomer structures with Rosetta 3.4 (39). We performed symmetry docking and predicted 10,000 tetramer structures for each molecule. Among the predicted structures, the structure with the best total score was selected as the model of the respective molecules. We compared the predicted tetramer structure of the MN4/LSDQ Vpu TM domain with the nuclear magnetic resonance (NMR) structure of the tetramer of the HIV-1_{BH10} Vpu TM domain (PDB accession number 1PI8). Their overall structures were highly similar. The root mean square deviation of C-α atoms between them was 1.64 Å.

RESULTS

Sequence homology- and structure-based modifications led to the identification of HIV-1mt CA residues that are responsible for the enhancement of viral growth in RhM cells. TRIM5 proteins inhibit retroviral infection in a species-specific manner. The RhM *TRIM5* coding sequence is highly polymorphic, and common RhM *TRIM5* alleles (*Mamu-1* to *Mamu-7*) can be divided into three groups based on polymorphisms at amino acid positions 339 to 341 within the B30.2/SPRY domain: $TRIM5^{TFP}$ (*Mamu-1* to *Mamu-3*), $TRIM5^{Q}$ (*Mamu-4* to *Mamu-6*), and $TRIM5^{CypA}$ (*Mamu-7*) (35, 40, 41). CyM TRIM5α has a Q residue at the corresponding site ($TRIM5^{Q}$), and CyM TRIM5CypA has a CypA sequence slightly different from that of RhM TRIM5CypA (42, 43). RhM and CyM TRIM5α proteins encoded by $TRIM5^{TFP}$ and $TRIM5^{Q}$ inhibit HIV-1 infection. On the other hand, CyM TRIM5CypA, but not RhM TRIM5CypA, restricts HIV-1 replication (42, 43). We have shown previously that a CXCR4-tropic MN4Rh-3 clone evaded CyM TRIM5CypA but was susceptible to TRIM5α restriction (19) and that its replication in *TRIM5*α homozygous CyM PBMCs/individuals was strongly restricted (24). Similarly, MN4Rh-3 replicated quite well in a CyM HSC-F cell line ($TRIM5^{Q/CypA}$) but very poorly in an RhM M1.3S cell line

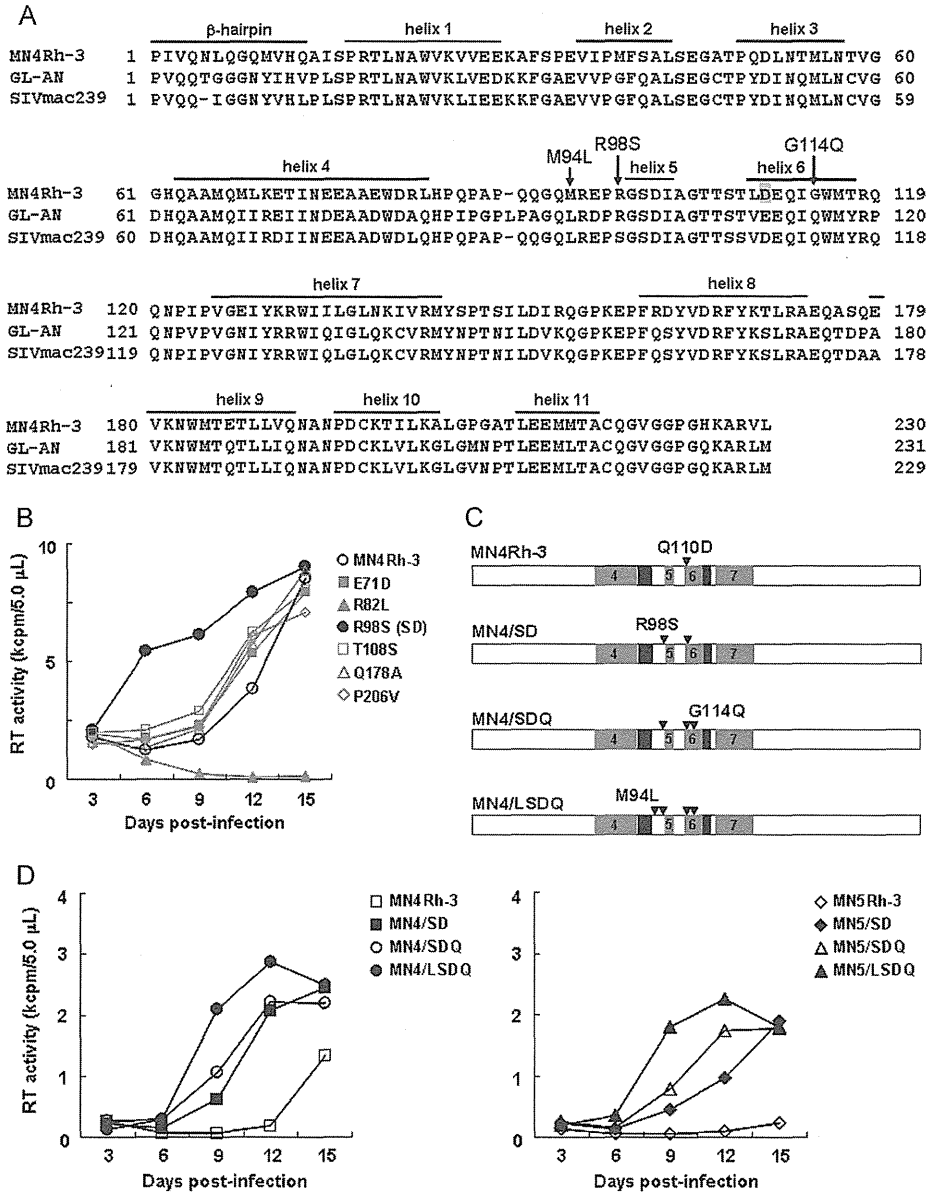

FIG 2 Identification of amino acid residues in HIV-1mt CA that are critical for viral growth enhancement in macaque cells. (A) Alignment of Gag-CA sequences. CA amino acid sequences of HIV-1mt MN4Rh-3 (19, 24), HIV-2 GL-AN (72), and SIVmac239 MA239 (71) are aligned. The N-terminal β-hairpin and helices 1 to 11 are indicated based on previously reported analyses (50, 73). The CA-Q110D mutation in MN4Rh-3 (19, 24) is shaded. Substitutions of three amino acids that contribute to the enhancement of HIV-1mt growth in macaque cells, described in this work, are indicated by arrows. (B) Growth kinetics of a parental clone, MN4Rh-3, and its CA mutants carrying a single-amino-acid change (see Table 1 for the mutants). Viruses were prepared from 293T cells transfected with the proviral clones indicated, and equal amounts (2×10^6 RT units) were inoculated into M1.3S cells (3×10^5 cells). Virus replication was monitored by RT activity released into the culture supernatants. Representative data from two independent experiments are shown. (C) Schematic CA structure of HIV-1mt clones. Amino acid substitutions are indicated in the order in which they were introduced into HIV-1mt CA. Black areas show sequences from SIVmac239. Helices 4 to 7 are shown as gray areas with the helix number. (D) Growth kinetics of CXCR4-tropic (left) and CCR5-tropic (right) HIV-1mt clones with different CA proteins (see reference 19 for CCR5-tropic MN5Rh-3). Viruses were prepared from 293T cells transfected with the indicated proviral clones, and equal amounts (2.5×10^6 RT units) were inoculated into M1.3S cells (10^6 cells). Virus replication was monitored by RT activity released into the culture supernatants. Representative data from two independent experiments are shown.

(*TRIM5*$^{TFP/TFP}$) (data not shown). Besides being a TRIM5α target, Gag-CA functions in various viral replication steps (44, 45). We thus used the M1.3S cell line as a target for multicycle infection to screen viral clones with increased replication potential following CA mutagenesis.

Modifications of MN4Rh-3 CA were performed based on sequence homology and structural modeling. As shown in Fig. 2A, the amino acid sequence identity of CA between HIV-1 and SIVmac239 is not high (~67% for SIVmac239 versus HIV-1_{NL4-3} and ~72% for SIVmac239 versus MN4Rh-3), but sequences are

relatively well conserved between HIV-2 and SIVmac239 (~90% for SIVmac239 versus HIV-2_{GL-AN}). Nevertheless, macaque TRIM5α restricts HIV-1 and HIV-2 infection but not SIVmac239. This distinct susceptibility to macaque TRIM5α results from the different CA sequences of each virus. We first selected amino acid residues in MN4Rh-3/HIV-2_{GL-AN} CA that are different from those of SIVmac239 CA and replaced these target residues with those of SIVmac239 (Table 1, MN4/SD and initial screening). The resultant clones were examined for their growth potential in M1.3S cells (Fig. 2B and Table 1). Of 25 clones tested, only MN4Rh-3 carrying an R98S change in CA (MN4/SD) exhibited enhanced viral growth efficiency (Table 1 and Fig. 2B). We previously found a growth-enhancing mutation, G114E, in CA by HIV-1mt adaptation in macaque cells (19). Since viral replication efficiency was decreased by the introduction of G114E into MN4Rh-3 (data not shown), we introduced an SIVmac239 CA-type G114Q mutation into the MN4/SD clone, and the resultant clone was designated MN4/SDQ (Fig. 2C and D). Moreover, we predicted an additional mutation that might improve the growth ability of MN4Rh-3 in macaque cells. Using HIV-2 CA, we previously found a key role of hydrogen bond formation between D97 within H4/5L (a loop between helices 4 and 5) and R119 within H6/7L (a loop between helices 6 and 7) in determining viral sensitivity to TRIM5α: TRIM5α-sensitive CA had a common H4/5L conformation with a decreased probability of hydrogen bond formation (46). The corresponding hydrogen bond was predicted to be formed between E96 in H4/5L and R118 in H6/7L of the MN4Rh-3 CA NTD. We assumed that the simultaneous introduction of SIV-CA-like amino acid residues at M94 in H4/5L and G114 in helix 6 might imitate the structural property of the SIVmac239 CA NTD surface for TRIM5α resistance and might be beneficial to improve the growth ability of MN4Rh-3 in macaque cells. The M94 residue is located in H4/5L, protruding its side chain near the G114 residue in helix 6. We therefore generated MN4/SDQ carrying the M94L mutation (MN4/LSDQ) (Fig. 2C and D). Three-dimensional locations of M94L, R98S, Q110D, and G114Q in the CA NTD are shown in Fig. 3. In addition, we constructed a series of CCR5-tropic viruses (MN5Rh-3, MN5/SD, MN5/SDQ, and MN5/LSDQ) (Fig. 2D), which carry the Env sequence derived from NF462 and a growth-enhancing Env S304G mutation (47). The growth potential of these viruses in M1.3S cells was analyzed. As shown in Fig. 2D, viral growth potential was enhanced with increasing amino acid substitutions in CA. MN4/LSDQ and MN5/LSDQ exhibited the highest replication potential in M1.3S cells in each group.

We constructed numerous HIV-1mt clones carrying CA mutations, including those described previously (48–50). All CA mutations and the growth potentials of the mutant viruses are summarized in Table 1. In the mutants derived from four HIV-1mt clones (MN4Rh-3, MN4/SD, MN4/SDQ, and MN4/LSDQ), most amino acid substitutions gave neutral or negative effects: CA amino acid substitutions that did not alter replication efficiency (L6I, E71D, T108S, Q178A, and P206V) or those that strikingly reduced the growth potential (e.g., Q50Y, T54Q, K70R, R82L, and L83Q; more than two consecutive mutations; and mutations in the β-hairpin domain). All listed HIV-1mt clones produced a significant amount of virions from transfected 293T cells, but none of them displayed a higher replication potential than MN4/LSDQ in M1.3S cells. In sum, M94L/R98S/G114Q substitutions in CA contributed to the growth enhancement of MN4Rh-3 in macaque cells.

Prediction of the effects of amino acid substitutions on the stability of the HIV-1 CA NTD. To investigate whether the M94L, R98S, Q110D, and G114Q mutations in MN4Rh-3 CA influenced the structural property of the protein, we analyzed the changes in stability by the mutations using the Protein Design application in MOE. The changes in stability by each of the point mutations M94L, R98S, Q110D, and G114Q were −0.41, 0.09, 0.25, and −1.70 kcal/mol, respectively (Fig. 3). The data suggested distinct effects of the single mutations at positions 94, 98, 110, and 114 on the stability of the HIV-1mt CA NTD. The Q110D mutation was predicted to destabilize the CA NTD. The R98S mutation has a similar negative effect on structure but to a much lesser extent. These mutations are considered to be more or less disadvantageous in terms of the CA structure. Nevertheless, they were critical for HIV-1mt growth enhancement in macaque cells (19) (Table 1 and Fig. 2). Therefore, these mutations must have given essential functions to CA protein in viral replication, which surpassed the structural disadvantage. On the other hand, M94L and G114Q mutations were predicted to stabilize the CA NTD. Therefore, these mutations may function as compensatory mutations that can redress structural disadvantages caused by R98S and Q110D mutations and increase growth ability in macaque cells. Our experimental data on MN4Rh-3, MN5Rh-3, and their derivatives having R98S/Q110D mutations, R98S/Q110D/G114Q mutations, and M94L/R98S/Q110D/G114Q mutations (Fig. 2) are consistent with this possibility.

Enhancement of viral replication efficiency by introduction of CA mutations (M94L/R98S/G114Q) correlates well with increased resistance to TRIM5α restriction. Some particular CA alterations (M94L/R98S/G114Q) of MN4Rh-3 markedly promoted viral replication in M1.3S cells with $TRIM5^{TFP/TFP}$ (Fig. 2D). Since TRIM5 proteins are potent restriction factors as species barriers (4, 8, 10) and can affect SIV transmission/replication *in vivo* (40, 51), it was expected that CA mutations (M94L/R98S/G114Q) would increase TRIM5α resistance as well as viral growth potential. To examine the effect of CA alterations on TRIM5α resistance, we carried out TRIM5α susceptibility assays using the recombinant SeV-TRIM5α expression system (36). TRIM5α resistance, as determined by this system, has been shown to be well reflected in the viral growth potential in macaque PBMCs/individuals due to the higher expression level of TRIM5α than that in feline CRFK cells stably expressing TRIM5α (19, 24). Four HIV-1mt clones (MN4Rh-3, MN4/SD, MN4/SDQ, and MN4/LSDQ) were assayed for their resistance to RhM-TRIM5α ($TRIM5^{TFP}$) and CyM-TRIM5α ($TRIM5^{Q}$), using SIVmac239 as a positive control. As shown in Fig. 4, the growth kinetics of SIVmac239 in cells expressing RhM- or CyM-TRIM5α or control B30.2/SPRY(−) TRIM5 were similar. Consistent with a previous analysis (19), MN4Rh-3 replication was strongly restricted in both RhM- and CyM-TRIM5α-expressing cells relative to that in control cells. Of note, TRIM5α resistance of MN4/SD, MN4/SDQ, and MN4/LSDQ quite paralleled their growth ability in M1.3S cells (see Fig. 2D for virus growth). While TRIM5α resistance of MN4/SD was increased relative to that of MN4Rh-3, MN4/SDQ exhibited higher resistance, especially to CyM-TRIM5α, than MN4/SD. MN4/LSDQ, which has the highest growth potential among the four HIV-1mt clones, showed the highest level of TRIM5α resistance, especially to RhM-TRIM5α. The HIV-1mt

TABLE 1 HIV-1mt CA mutants constructed in this study

Clone designation	CA mutation(s)[b]	Growth potential[c]
MN4Rh-3[a]	None (parental clone)	++
MN4/SD	R98S	+++
MN4/SDQ	R98S, G114Q	+++
MN4/LSDQ	M94L, R98S, G114Q	++++
Initial screening		
E71D	E71D	++
R82L	R82L	−
RL82LQ	RL82, 83LQ	−
T108S	T108S	++
Q178A	Q178A	++
P206V	P206V	++
PD	L6P	−
PDQ	L6P, G114Q	−
PYD	L6P, Q50Y	+
PYDQ	L6P, Q50Y, G114Q	+
PYQD	L6P, Q50Y, T54Q	+
PYQDQ	L6P, Q50Y, T54Q, G114Q	+
GG	LQ6, 7GG	−
GG-T117Y	LQ6, 7GG, T117Y	−
IGGN	LQGQ6-9IGGN	−
IGGN-T117Y	LQGQ6-9IGGN, T117Y	−
5IGGN	NLQGQ5-9IGGN	−
YD	Q50Y	−
YDQ	Q50Y, G114Q	−
YQD	Q50Y, T54Q	−
YQDQ	Q50Y, T54Q, G114Q	−
IIRDI	MLKET68-72IIRDI	−
TDA	ASQ176-178TDA	−
VNP	PGA206-208VNP	−
Mutants from MN4/SD		
L6I-S	L6I, R98S	++
YQ-S	Q50Y, T54Q, R98S	−
DS	E71D, R98S	+++
SS	R98S, T108S	+++
SA	R98S, Q178A	+++
SV	R98S, P206V	+++
SAV	R98S, Q178A, P206V	+++
DSAV	E71D, R98S, Q178A, P206V	+++
Mutants from MN4/SDQ or MN4/LSDQ		
L6I-LSDQ	L6I, M94L, R98S, G114Q	++++
YQ-LDQ	Q50Y, T54Q, M94L, G114Q	−
YQ-SDQ	Q50Y, T54Q, R98S, G114Q	−
YQ-LSDQ	Q50Y, T54Q, M94L, R98S, G114Q	−
K70R-LSDQ	K70R, M94L, R98S, G114Q	−
E71D-LSDQ	E71D, M94L, R98S, G114Q	+++
E79D-LSDQ	E79D, M94L, R98S, G114Q	++++
R82L-LSDQ	R82L, M94L, R98S, G114Q	−
L83Q-LSDQ	L83Q, M94L, R98S, G114Q	−
T108S-LSDQ	M94L, R98S, T108S, G114Q	++++
E79D-T108S-LSDQ	E79D, M94L, R98S, T108S, G114Q	++++
E127N-LSDQ	M94L, R98S, G114Q, E127N	+++
I134Q-LSDQ	M94L, R98S, G114Q, I134Q	−
LSDQN	M94L, R98S, G114Q, S148N	−
I152V-LSDQ	M94L, R98S, G114Q, I152V	+++
LSDQA	M94L, R98S, G114Q, Q178A	++++
IY-LSDQA	L6I, M10Y, M94L, R98S, G114Q, Q178A	++
YQ-LSDQA	Q50Y, T54Q, M94L, R98S, G114Q, Q178A	−
LSDQA-P159S	M94L, R98S, G114Q, P159S, Q178A	+++

(Continued on following page)